Removal of ^{137}Cs from ecosystems using phytoremediation in former Soviet Union

（旧ソ連邦におけるファイトレメディエーションを用いた
放射性 ^{137}Cs 除去技術の確立）

Final Report on Research Project
(Number: 13574019)
under Grant-in Aid for Scientific Research (B)(2)
for 2001 to 2002
from
Ministry of Education, Culture, Sports, Science and Technology

Shinya FUNAKAWA
Associate Professor
Graduate School of Agriculture

March 2004

Acknowledgement

This research is supported by many researches, especially in the field sampling in former Soviet Union.

First of all, I am deeply grateful to Professor Dr. Nikolai I. Pulupan, who kindly guided us for extensive field survey in Ukraine.

I wish to express my sincere gratitude to Dr. Takashi Kosaki, Professor of Kyoto University, for his guidance and the valuable discussions.

I also wish to express my appreciation for the staff members of the Institute for Soil Science and Agrochemistry Research for their kind assistance for our field survey.

Shinya Funakawa
Graduate School of Agriculture
Kyoto University

[研究組織]

研究代表者	舟川晋也	京都大学大学院・農学研究科・助教授
研究分担者	矢内純太	京都大学大学院・地球環境学堂・助手
海外共同研究者	Konstantin Pachikin	カザフスタン国国立土壌研究所・主任研究官
	Vadim Solovey	ウクライナ国国立農芸化学・土壌研究所・主任研究官
（研究協力者	渡邉哲弘	京都大学大学院・農学研究科
	中尾　淳	京都大学大学院・農学研究科）

[交付決定額]　(配分額)

（金額単位：千円）

	直接経費	間接経費	合　　計
平成 13 年度	4,700	0	4,700
平成 14 年度	2,200	0	2,200
総　　計	6,900	0	6,900

[研究発表]

（学会誌等）

Funakawa, S., Ashida, M., and Yonebayashi, K. 2003: Charge characteristics of forest soils derived from sedimentary rocks in Kinki District, Japan, in relation to pedogenetic acidification process. *Soil Sci. Plant Nutr.*, 49(3), 387-396.

Yanai, J., Mabuchi, N., Moritsuka, N., and Kosaki, T. 2004: Changes in the distribution and forms of cadmium in the rhizosphere of Brassica juncea in Cd contaminated soils and its implication to phytoremediation *Soil Sci. Plant Nutr.*, 50, (in press).

（学会発表）

Nakao, A., Funakawa, S., and Kosaki, T. : Kinetics of Cs adsorption on soils with different mineralogical compositions, International Symposium on Radioecology and Environmental Dosimetry, October 23, 2003

渡邉哲弘，舟川晋也，小崎隆：湿潤洗脱条件下における膨張性 2：1 型土壌粘土鉱物生成条件の検討，日本土壌肥料学会 2002 年度大会（東京）、2002 年 4 月 3 日

渡邉哲弘，小川菜穂子，舟川晋也，小崎隆：土壌酸性化中和要因の反応速度論的解析，日本土壌肥料学会 2003 年度大会（東京）、2003 年 8 月 20 日

Contents

Chapter 1
Introduction

1.1 ^{137}Cs fallout after Chernobyl accident

^{137}Cs is one of the main radioisotopes that have been released into the environment so far by nuclear powerstation accidents and nuclear weapons tests. In 1986, the explosion of a nuclear power plant happened at Chernobyl in former Soviet Union, and huge amount of radionuclides were deposited over large areas of Europe. From the radiological point of view, ^{131}I and ^{137}Cs are the most important radionuclides after the accident, because they are responsible for the most of radiation exposure to human beings. The half-life periods of ^{131}I and ^{137}Cs are 8 days and is about 30 years, respectively. Therefore during a few weeks after the Chernobyl accident, both of gamma and beta radiations were mainly emitted from ^{131}I and attacked to humans intensively, while influence of ^{137}Cs is still continuing even at present. The contamination of ^{137}Cs in farmland is a particularly serious problem because it would result in the inner exposure of humans through contaminated food products.

The most highly contaminated area is a 30-km zone surrounding the reactor, where ^{137}Cs depositions in soils generally exceeded 1500 kBq m^2 (Henri 2002). People living there were forced to immigrate to another place by the government.

1.2 Slow migration rate of ^{137}Cs

After the Chernobyl accident, a lot of field studies have been conducted in several European countries. Most of the studies have concluded that ^{137}Cs tends to remain within upper layers of soils and, in a large variety of soils, ^{137}Cs migration rates were found to be quite slow. For example, in Swedish soil profile, 50-92% of the ^{137}Cs fallout was still present in the upper 5-cm layers, and the migration rate of ^{137}Cs ranged between 0.2 and 1.0 cm year^{-1} (Rosen et al., 1999). In Italy, Livens et al. (1996) found that more than 90% of the ^{137}Cs was retained in the upper 10 cm of 10 different soils in semi natural upland areas. In Belarus, Knatko et al. (1996) found that 90% of the ^{137}Cs were remaining at the upper 5 cm in two types of sandy soils and at the upper 10 cm in a sod-podzolic sandy soil. All these findings indicate vary slow migration rates of ^{137}Cs in soils and strongly suggest an importance of strategy that directs to remove ^{137}Cs from upper layers of soils directly, not by leaching to downward. Phytoremediation, by which ^{137}Cs can be removed from soils into plant bodies, is one of trials for such a direction.

The migration and distribution of ^{137}Cs in soil profile vary depending on soil properties such as mineralogy, soil texture, organic matter content and pH, as well as on climate conditions, land use and management practices. Above all, mineralogy (i.e. composition of

clay minerals) is the most important factor that governs ^{137}Cs mobility through specific adsorption onto negatively charged colloidal surfaces.

1.3 Objectives of this study

In order to establish available strategy for minimizing ^{137}Cs contamination into food products or for removing ^{137}Cs using phytoremediation, it is necessary to understand Cs^+ adsorption / desorption behavior as well as Cs^+ transfer mechanism in soils.

Since the nature of 2:1 phyllosilicates, which are mainly responsible for Cs immobilization in soils, largely depend on weathering conditions of soils. Therefore it is useful to compare behaviors of Cs^+, i.e., adsorption to and desorption from soils, in different soils to choose an appropriate direction for remediation. Soils of Southeast Asia were selected as comparative samples with Ukrainian soils in this study, because they have been subjected to an extensive weathering under climates with much more annual precipitations and relatively higher annual temperature than Ukraine. According to reports in the past, such 2:1 phyllosilicates as dominated by octahedral isomorphic substitutions have no Cs immobilizing capacity. This concept should be verified because most Ukrainian soils are expected to exhibit few specific adsorptions against Cs^+, judging from their mineralogical compositions, in spite of the fact that Ukrainian soils have retained ^{137}Cs within surface layers of soils over 10 years. In addition, difference of Cs immobilizing mechanisms between frayed edge sites of weathered mica, or illite, and collapsed interlayers of expandable 2:1 minerals has not been cleared.

In this study, we firstly analyze weathering processes of 2:1 layer silicates including transformation of 2:1 minarals and neoformation of kaolinite and gibbsite under different geological and bio-climatic conditions in humid Asia (Chapter 2). The soils from Ukraine are excluded from this analysis because the climatic condition there is not assumed to accelerate mineral weathering. Then, in Chapter 3, we will comparatively assess the Cs immobilizing capacity as well as time dependent processes of Cs^+ adsorption / desorption reactions on soils from Ukraine and Asian countries using both a batch technique and a continuous flow methods.

Chapter 2
Clay mineral formation under different weathering environments in humid Asia

2.1 General

In order to know inherent soil fertility for appropriate land management in relatively large scales, it is indispensable to understand general trend of distribution patterns of clay minerals in relation to geological and/or weathering conditions. Such information is, however, still scarcely available in humid tropics in Asian countries (Yoshinaga et al. 1989; Araki et al. 1990; Ohta and Effendi 1992). It is necessary to fill the gap of information.

Because of the importance of soil clay minerals, many experiments and surveys are conducted on weathering / formation processes of minerals and their thermodynamic stability in both laboratories and fields. Transformation of mica is most important for the formation of expandable 2:1 type clay minerals such as vermiculite and smectite. Mica is usually a primary mineral and does not form in soils except for a few cases, e.g., mica formation from vermiculite under a high K concentration reported by Nettleton et al. (1973). Mica weathers or transforms to vermiculite that is rarely contained in parent rocks, with a decreasing layer charge and releasing interlayer alkaline metals. Further reduction of the layer charge results in formation of smectite (Fanning et al. 1989). Kittrick (1973) investigated thermodynamic stability of trioctahedral vermiculite and concluded that trioctahedral vermiculite was unstable under natural soil environment. Dioctahedral vermiculite is more common in soils (Kittrick 1973; Jackson 1959) and is thought to be more stable than trioctahedral one (Barshad and Kishk 1969), thermodynamic data of this mineral is not yet reported. The stability of dioctahedral vermiculite is. In acidic soils hydroxy-Al interlayered vermiculite (HIV) forms and it seems to be as stable as gibbsite and kaolinite because of the presence of interlayered materials. (Karathanasis et al.1983; Carlisle and Zelazny 1973; Zelazny et al. 1975). Gibbsite is believed to form only under conditions of strong desillication, where H_4SiO_4 activity is very low, while kaolinite forms in moderate H_4SiO_4 activity. Generally leaching condition, temperature, parent rock, topography, ground water table, vegetation and time factor control the H_4SiO_4 activity (Huang et al. 2002). Smectite has multiple origins; it may be neoformed from soil solution under high Si activity conditions, originally contained in certain parent materials, or transformed from mica or vermiculite as stated earlier (Reid-Soukup and Ulery 2002).

The mineral weathering sequences in humid Asia are, however, not fully understood in spite of many researches introduced above because most of the studies have been conducted in another continents. Soils in Asia are generally much younger than the other regions mainly because of geological (i.e., a lot of volcanoes) and/or topographical (i.e., influence of Alpine

orogene) reasons. The objective of this study is, therefore, to reveal the difference in forming processes of clay minerals and their stabilities under various weathering conditions in humid Asia based on mineralogical and thermodynamic analyses. Especially the latter approach helps to explain mineral weathering / formation phenomenon theoretically and to predict present and future distribution of clay minerals (Van Breemen and Brinkman 1976; Karathanasis 2002; Rai and Kittrick 1989; Wolt 1994).

2.2 Materials and methods

2.2.1 Soil samples

Soil samples were collected from residual slopes of East and Southeast Asia, namely Japan, Indonesia including Java, Sumatra and Kalimantan islands, and Thailand. They involve various parent materials and climatic regimes (Fig. 2.1).

Parent materials of the soil samples are shown on Table 2.1. Japan is a part of the circum-pacific volcanic belt and volcanic materials (i.e., tephra), felsic igneous rocks and sedimentary rocks are widely distributed. Parent materials of our samples involve shale, granite, rhyolite and gabbro. Except for gabbro, parent rocks contain an appreciable amount of mica that can weather to expandable 2:1 type minerals. West part of Thailand is the end of the Alpine orogene. Parent rocks include granite and sedimentary rocks and most of them contain mica. Geology of Indonesia is different for each island. Java is a part of the volcanic belt and soils are affected more or less by volcanic ejecta. Parent materials of the samples from Java are tephra, andesite, and sedimentary rocks including limestone. Most of the volcanic materials are mafic, and felsic rocks are distributed only in limited area. Western part of Sumatra is also a part of the volcanic belt, while central to eastern parts are covered with sedimentary or metamorphic rocks or peat deposit. Parent materials of Sumatra samples are tephra, granite and sedimentary rock. East Kalimantan is very different from these two islands. Most of the island is covered with sedimentary rocks and there is no volcano.

The temperature and moisture regimes of the areas are shown in Fig. 2.1, together with their mean annual values of representative sites. All the soils collected have formed in humid climates. We excluded soils on poorly drained condition from this study, because they were supposed to be formed under quite different weathering environment. Temperatures of Indonesia and Thailand are higher than those of Japan thus chemical reactions occur quickly and it may be easier to form more crystalline minerals. On the other hand, in Japan organic matter tends to accumulate in soils, which may retard rapid crystallization of clay minerals (Hirai et al. 1991). Precipitations of Japan, East Kalimantan, Sumatra and West Java are large as mostly exceeding 2000 mm, while Thailand and East Java have a distinct dry season and precipitations are smaller than the others.

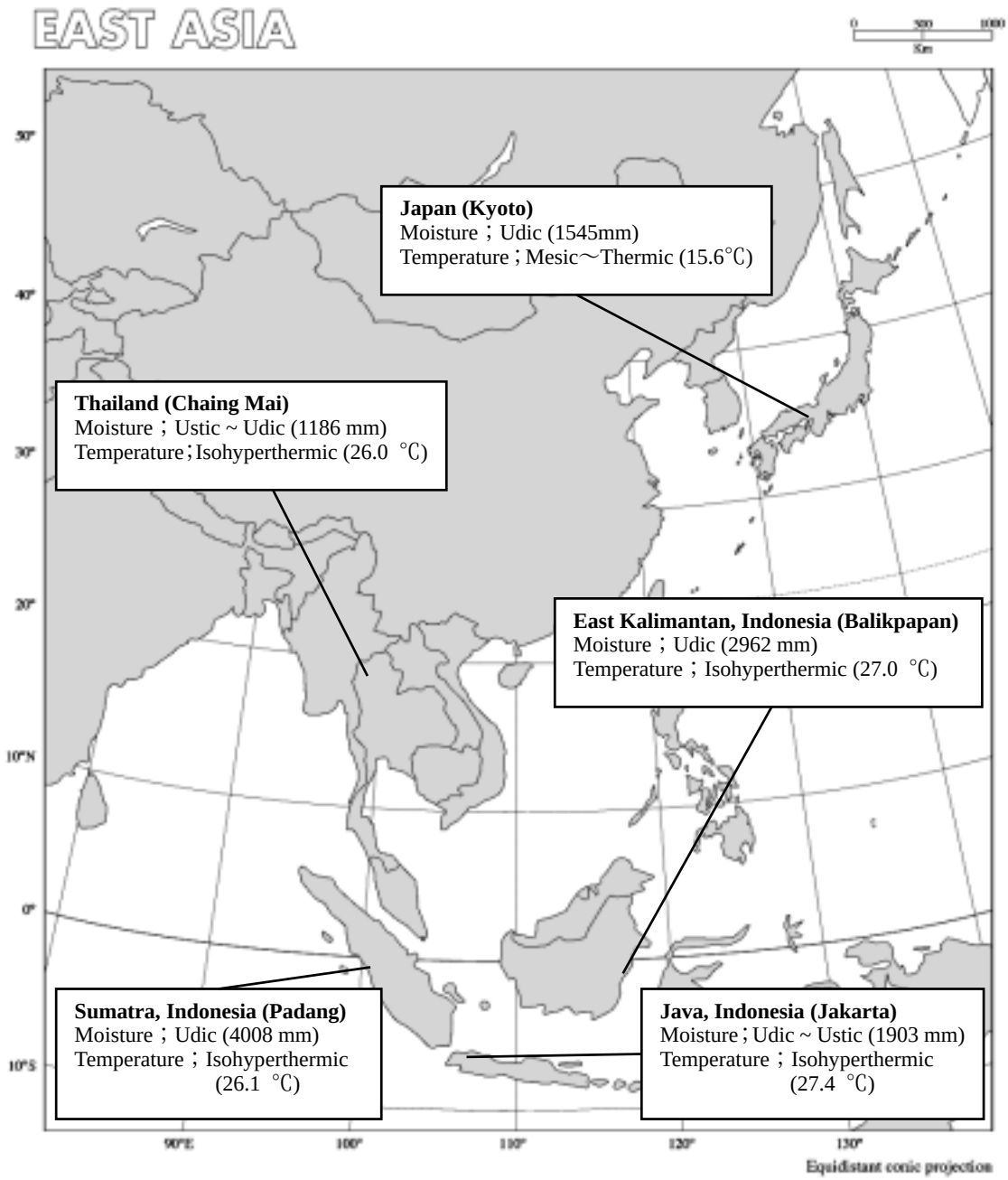

Fig. 2.1. Study sites.

2.2.2 Analytical methods

Subsurface soils were used in this study. Before the experiments these soils were air-dried and crushed to pass through a 2 mm mesh sieve.

The pH was measured with a glass electrode using a soil to solution (H_2O or 1 M KCl) ratio of 1 to 5. Exchangeable cations (Ca^{2+}, Mg^{2+}, Na^{+}, K^{+} and NH_4^{+}) and CEC were measured using ammonium acetate (1 M and pH 7) as an electrolyte. Total carbon and nitrogen contents were determined by the dry combustion method with NC analyzer (Sumika

Chemi. Anal. Service, SUMIGRAPH NC-800-13N). For particle size distribution, the coarse and fine sand fractions were determined by sieving and the silt and clay fractions by the pipette method after decomposition of organic matter with H_2O_2 and complete dispersion with an addition of NaOH and ultrasonic treatment.

Mineral compositions of clay and silt fractions, which were collected during the particle size analysis, were identified with X-ray diffraction (XRD) after different treatments, i.e. Mg-saturation (air dried), glycerol solvation after Mg-saturation, and K-saturation (air dried and heated to 350℃ and 550℃) using X-ray diffractometer (Rigaku, RAD-2RS; Cu-Kα radiation, 30 kV and 20 mA). The amounts of gibbsite and kaolinite in the clay fraction were determined with differential thermal analysis and thermalgravimetry, respectively, using simultaneous DTA-TG apparatus (Shimazu, DTG60; rate of temperature rise being set at 20℃ min^{-1}) after removal of iron hydroxides by citrate-dithionite-bicarbonate (pH 7.3) treatment at 80℃. The amounts of noncrystalline aluminosilicates and hydrous oxides (Alo, Sio and Feo), which were extracted with acid ammonium oxalate (0.2 M and pH 3.0) in the dark, were measured with inductively coupled plasma atomic emission spectrometer (ICP-AES, Shimazu, SPS1500VR).

Quasi-soil-solution were collected after continuous shaking for 1 week at 25℃ and 1 atm with soil to water ratio of 1 to 2 and filtrated through a 0.025 μm millipore filter before the analyses. H^+ and F^- activities were determined with glass electrodes. The concentrations of Na^+, K^+, NH_4^+, Cl^-, NO_3^-, and SO_4^{2-} were measured with high performance liquid chromatography (Shimazu, Ion chromatograph HIC-6A equipped with conductivity detector CDD-6A and shim-pack IC-C3 for cations and shim-pack IC-A1 for anions). The concentrations of Si, Ca, Mg, Fe, Mn, Ti and Al were determined with ICP-AES (Shimazu SPS1500VR). The amount of Al that was not adsorbed on partially neutralized (pH 4.2) cation exchange resin (Amberlite IR-120B(H)) in a column was determined with ICP-AES (Shimazu SPS1500VR) and assigned to Al complexed with organic matter. The difference between Al concentrations determined without and with the column treatment, or the fraction retained on the cation exchange resin, was assigned to inorganic monomeric Al. The resin treatment was run according to the scheme developed by Hodges (1987). The amount of inorganic carbon and total organic carbon were determined with total organic carbon analyzer (Shimazu, TOC-V CSH). The activity of each ion was calculated with the measured concentrations according to Adams (1971).

2.3 Results

2.3.1 Mineral composition in silt and clay fractions

The samples are divided into 4 groups, i.e., those from Japan (JP), Thailand (TH), sedimentary rocks in Indonesia (ID-S), and volcanic materials in Indonesia (ID-V). Physicochemical properties of selected samples are shown in Table 2.1. Clay mineral compositions were determined semi-quantitatively by XRD (Fig. 2.2). The relative peak area of 1.4 nm, 1.0 nm (mica) and 0.7 nm (kaolin) minerals in the diffractograms are plotted on Fig. 2.3 and for representatives shown in Table 2.2.

Table 2.1. General physicochemical properties of the soils studied.

					General physicochemical properties										
	Sample name	Horizon	Depth cm	Parent rock	pH(H_2O)	pH(KCl)	TC %	CEC cmol (+) L^{-1}	ex. Ca cmol (+) L^{-1}	ex. Mg cmol (+) L^{-1}	ex. K cmol (+) L^{-1}	ex. Na cmol (+) L^{-1}	sand %	silt %	clay %
JP	EG1	AB	8-17	Rhyolite	4.8	3.6	0.7	9.7	0.41	0.34	0.16	0.06	56	25	19
		BC	30-40		5.0	3.6	0.3	9.3	0.49	0.23	0.18	0.06	55	23	22
	EG2	AB	9-20	Rhyolite	4.6	3.7	1.1	14.4	0.08	0.00	0.15	0.06	39	25	35
		BC	33-45		4.6	3.9	0.4	11.8	0.00	0.00	0.11	0.07	57	15	28
	FJ	B1	7-20	Granite	4.4	3.9	3.1	13.6	0.00	0.00	0.17	0.07	57	17	27
		BC	32-42		4.5	4.1	0.7	8.6	0.00	0.00	0.12	0.05	61	12	27
	TN100	CB1	4/7-32/39	Granite	4.9	4.2	0.9	6.7	0.00	0.00	0.17	0.08	66	15	19
		CB1	55/65-92		5.1	3.9	0.1	5.2	0.16	0.00	0.14	0.09	70	13	16
	KS	AB	6-12	Gabbro	4.3	3.7	4.5	23.5	0.74	0.34	0.19	0.08	22	33	45
		Bw	23-39		4.5	3.8	1.2	19.1	0.16	0.00	0.10	0.07	23	31	46
	AS	E	2.5-11	Shale	3.5	3.2	3.0	18.5	0.00	0.00	0.14	0.09	31	26	43
		B	11-27		3.8	3.7	3.9	26.5	0.00	0.00	0.22	0.10	32	23	45
	SD	AB		Volcanic Ejecta	5.0	4.6	9.4	31.9	0.16	0.00	0.16	0.04	38	27	35
TL	RP-C3		10-20	Sedimentary Rock	6.5	5.0	1.8	19.5	3.62	2.23	0.48	0.03	32	22	46
			30-40		5.5	4.4	0.9	20.3	0.85	1.08	0.20	0.01	22	17	61
	HM-F1		10-20	Granite	5.5	4.1	0.9	7.9	0.05	0.69	0.23	0.01	60	15	26
			30-40		5.4	4.0	0.7	13.5	0.04	1.16	0.27	0.02	52	15	33
	MT-C1		30-40	Granite	5.5	4.1	0.8	13.9	0.51	1.24	0.60	0.02	43	12	46
	NS-C1		30-40	Shale	5.2	4.0	1.3	17.5	0.12	0.65	0.40	0.02	7	15	78
	HY-C2		30-40	Andesite	5.7	4.1	0.6	10.5	0.08	0.00	0.47	0.04	17	29	54
	R1080-F1		30-40	Sedimentary Rock	5.0	4.0	1.4	18.4	0.56	0.81	0.47	0.03	8	23	69
	R1148-F1		30-40	Sedimentary Rock	4.8	4.0	0.9	12.4	0.24	0.18	0.06	0.05	14	29	57
	KM-C1		30-40	Sedimentary Rock	5.2	4.0	8.6	20.1	0.16	0.68	0.18	0.04	10	14	76
	R1097-F2		30-40	Sedimentary Rock	5.4	4.0	1.1	14.6	0.48	0.29	0.53	0.02	10	25	65
	MD-F1		30-40	Sedimentary Rock	5.1	4.4	4.7	17.7	0.55	1.74	0.30	0.01	42	24	35
	R1080-F2		30-40	Sedimentary Rock	5.0	3.9	0.4	7.9	0.06	0.32	0.45	0.04	55	15	30
	RJ-C1		30-40	Granite	5.5	4.2	1.5	17.3	0.16	0.20	0.46	0.03	34	17	49
	MT-C2		30-40	Granite	5.5	4.3	1.0	9.6	2.39	0.73	0.31	0.02	53	16	32
ID-S	JV11	A	0-10	Sedimentary Rock	5.0	4.5	2.2	21.6	8.62	4.76	0.77	0.11	43	23	34
		R	10-40		5.5	4.4	0.7	17.4	7.34	3.56	0.64	0.11	62	18	20
	JV17	B1	3-30/35	Limestone	5.9	5.4	1.6	25.8	10.07	2.06	0.12	0.10	7	13	80
		B3	60+		5.5	5.0	1.4	29.9	13.52	2.35	0.11	0.12	7	14	79
	EK10	Be	3-20	Sedimentary Rock	3.9	3.8	1.3	11.9	0.24	0.46	0.35	0.06	33	31	36
		Btg	40-55		3.8	3.6	0.6	17.8	0.08	0.00	0.19	0.03	27	25	49
	EK11	Be	7-20	Sedimentary Rock	4.9	4.5	1.3	17.9	9.56	1.23	0.24	0.07	26	35	39
		Btg	40-50		4.5	3.8	0.7	18.8	8.45	0.90	0.21	0.03	18	30	52
	LB41		40-60	Sedimentary Rock	4.5	4.0	0.6	9.2	0.16	0.00	0.05	0.03	52	15	32
	KD01		20-40	Sedimentary Rock	4.7	4.0	0.9	14.6	0.03	0.01	0.15	0.03	34	27	38
	7		30-60	Sedimentary Rock	4.8	3.7	0.6	17.2	0.55	1.10	0.12	0.05	20	27	53
	31		30-60	Sedimentary Rock	4.6	3.4	1.5	21.5	4.28	3.25	0.19	0.07	5	28	67
	14		30-60	Sedimentary Rock	4.6	3.6	2.1	15.2	2.55	2.93	0.26	0.10	18	35	47
	28		30-60	Sedimentary Rock	4.4	3.8	0.4	18.2	0.44	0.18	0.11	0.06	34	21	45
	13		30-60	Sedimentary Rock	4.3	3.7	0.4	14.0	0.13	1.10	0.08	0.03	29	27	45
	SM4	B2t	35-55	Sedimentary Rock	4.3	3.9	0.7	14.2	0.08	0.00	0.11	0.02	20	30	50
ID-V	JV1	B	35-63	Volcanic Ejecta	5.3	3.9	0.5	40.0	3.24	19.16	0.13	0.13	48	19	33
	JV5	B1	5-45	Andesite	4.3	4.0	0.9	14.4	0.41	0.34	0.42	0.17	11	22	67
		B2t	45-60		4.3	4.0	0.7	19.7	0.08	0.23	0.30	0.10	9	18	73
	JV13	B1	6-19	Andesite	5.4	4.9	1.7	27.2	12.31	5.91	0.13	0.20	48	17	35
		B2t	19-35		5.2	4.6	0.8	34.0	9.47	6.48	0.12	0.35	26	10	65
	JV14	A	0-6	Andesite	6.5	5.5	1.7	26.1	21.81	4.19	0.15	0.14	82	13	5
		C	6-25		5.9	3.9	0.1	22.4	18.53	1.85	0.05	0.21	86	11	3
	SM6	BA	2-12	Granite	4.0	4.0	0.8	6.2	0.57	0.00	0.12	0.03	67	18	15
		B2	40-60		4.2	4.0	0.3	5.9	1.68	0.00	0.09	0.05	54	31	15
	SM10	B2t	30-55	Volcanic Ejecta	4.8	3.9	0.7	16.1	3.16	0.00	0.05	0.01	21	29	50
	SM13	B	11-30	Volcanic Ejecta	4.6	3.9	1.4	21.9	1.94	1.75	0.11	0.05	19	17	64

When mica peak at 1.0 nm is not detected in silt fraction, as in the most cases that the parent materials are mafic, such as KS, JV5, JV13, JV17, SM10, and SM13, neither mica nor vermiculite is detected in clay fractions. In this case mica minerals are assumed to be absent in parent materials and in soils kaolin and/or smectite are dominant clay minerals (e.g., ID-V in Fig. 2.2).

On the contrary, the soils of TH, JP and ID-S contain an appreciable amount of mica in silt fraction judging from a sharp mica peak at 1.0 nm. Among them, in clay fraction of TH, kaolinite is predominant and 1.4 nm minerals are mostly low as less than 20% (Fig. 2.3).

In both the JP and ID-S soils, not like as in TH, a fairly large amount of 1.4 nm minerals existed in clay fraction. Generally higher peaks of 1.4 nm minerals are detected in clay fraction than in silt fraction, suggesting that 1.4 nm clay minerals are formed from mica inherited from parent materials (Fig. 2.2). In JP, 1.4 nm minerals are identified with HIV or vermiculite. The former is generally found in lower horizons and the latter in upper horizons

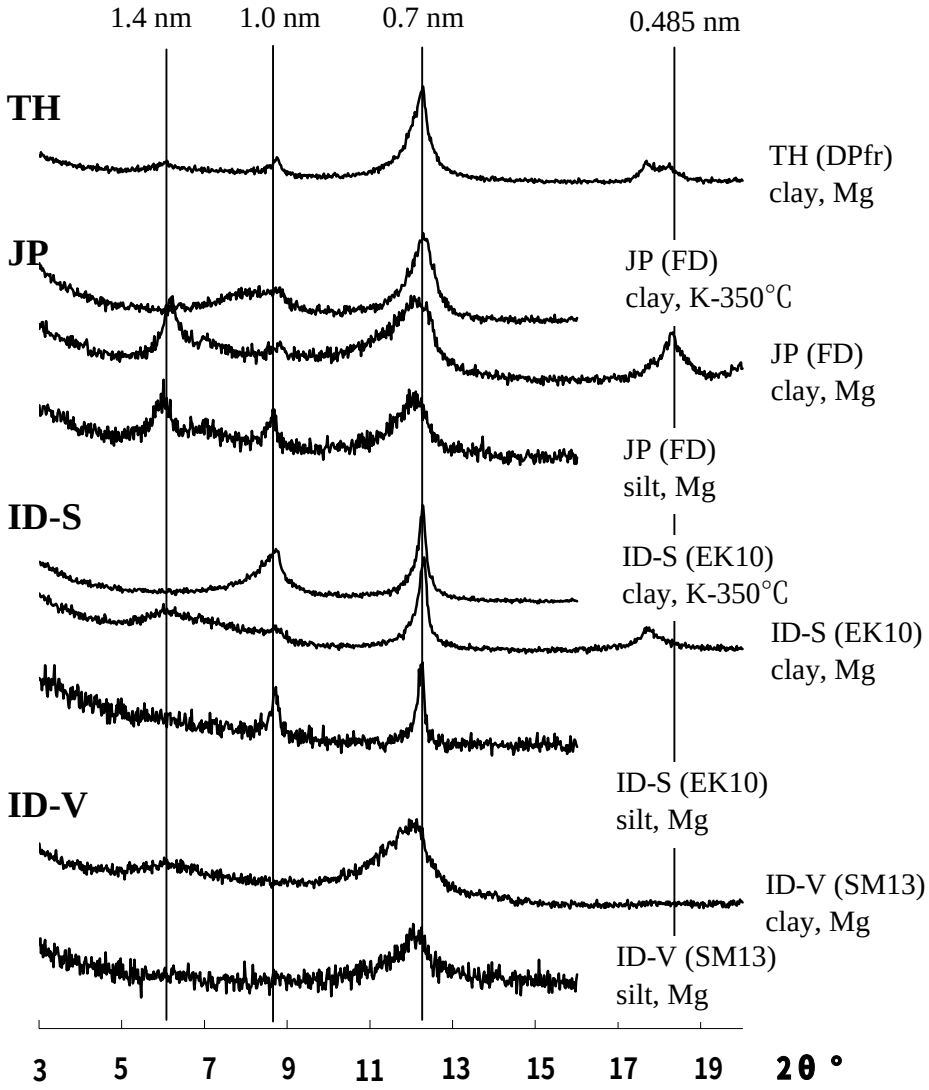

Fig. 2.2. X-ray (Cu-Kα) diffractograms from oriented specimens from silt and clay fractions.

in a soil profile. A broader peak at 0.7 nm among the JP samples indicates a lower crystallinity of kaolin minerals compared to ID-S and TH (Fig. 2.2). Gibbsite is also clearly detected in all the JP samples.

In ID-S, peaks at 0.7 nm (kaolin) and 1.4 nm are conspicuous. The 1.4 nm peak is derived either from vermiculite, smectite or HIV. In the case of HIV, the 1.4 nm peak collapse more easily with heating treatment than in JP, indicating interlayered materials are much less.

In JV1, JV11, and JV14, smectite dominates and this may be inherited from parent rocks judging from the presence of smectite in silt fraction.

The results of thermal analysis are plotted in Fig. 2.4 and for representatives given in Table 2.2. Distribution of gibbsite is very interesting. This mineral is usually thought to be distributed more in older soils, but in this study a large amount of gibbsite is contained in JP

Table 2.2. Composition of quasi-soil-solution and mineral composition of the soils.

				Quasi-soil-solution								Thermal analysis			XRD analysis		
	Sample name	Horizon	Depth cm	Al_O %	Si_O %	Fe_O	pH	log (H_4SiO_4)	log (Al^{3+})	log (Mg^{2+})	log (K^+)	gibbsite %	kaolin %	other minerals %	1.4 nm %	1.0 nm %	0.7 nm %
JP	EG1	AB	8-17	0.00	0.04	0.22	5.0	-3.2	-5.4	-4.7	-4.0	0.4	32.2	67.3	56	18	25
		BC	30-40	0.07	0.04	0.17	5.4	-3.1	tr.	-4.9	-4.0	0.6	45.7	53.6	50	28	21
	EG2	AB	9-20	0.28	0.04	0.34	4.6	-3.5	-4.8	-4.7	-4.2	0.6	48.4	51.0	53	3	44
		BC	33-45	0.30	0.06	0.22	4.6	-3.7	tr.	-4.9	-4.3	2.2	53.9	43.9	59	5	37
	FJ	B1	7-20	0.28	0.04	0.39	4.5	-3.3	tr.	-4.7	-3.8	6.5	64.5	29.0	40	10	50
		BC	32-42	0.37	0.07	0.11	4.6	-3.7	-4.9	-4.9	-4.1	10.7	65.7	23.6	23	14	63
	TN100	CB1	4/7-32/39	0.37	0.06	0.20	5.5	-3.5	tr.	-5.1	-4.0	25.2	52.1	22.8	50	5	46
		CB1	55/65-92	0.16	0.05	0.09	5.3	-3.4	tr.	-5.1	-4.5	11.1	55.3	33.6	49	8	43
	KS	AB	6-12	0.54	0.05	1.17	4.4	-3.5	tr.	-4.3	-4.1	1.1	69.8	29.0	24	1	75
		Bw	23-39	0.47	0.06	0.61	4.7	-3.8	tr.	-4.6	-4.8	2.0	67.9	30.1	34	4	62
	AS	E	2.5-11	0.23	0.03	0.56	3.7	-3.3	-4.0	-4.5	-4.0	1.2	16.5	82.3	65	30	5
		B	11-27	0.72	0.05	2.12	4.4	-3.5	-4.8	-4.8	-4.2	9.0	20.4	70.6	79	19	2
	SD	AB		4.66	1.31	1.94	5.4	-3.6	-6.5	-4.8	-4.2	0.8	n.d.	99.2	n.d.	n.d.	n.d.
TL	RP-C3		10-20	0.19	0.04	0.50	7.6	-3.8	-7.7	-3.9	-3.7	0.4	34.9	64.7	5	52	44
			30-40	0.00	0.06	0.49	6.5	-4.1	-6.9	-4.6	-4.7	0.5	38.0	61.5	7	45	48
	HM-F1		10-20	0.23	0.04	0.34	6.5	-3.3	tr.	-5.1	-4.0	0.3	59.8	39.9	2	27	70
			30-40	0.00	0.05	0.41	6.2	-3.6	tr.	-4.9	-4.2	0.2	63.6	36.2	0	20	80
	MT-C1		30-40	0.13	0.04	0.25	5.9	-3.6	tr.	-4.9	-3.8	0.4	63.4	36.2	1	14	86
	NS-C1		30-40	0.22	0.05	0.42	5.5	-4.2	-7.3	-5.1	-4.3	0.2	32.8	67.0	0	52	48
	HY-C2		30-40	0.18	0.04	0.25	5.8	-4.0	tr.	-6.3	-4.1	0.4	48.6	51.0	0	35	65
	R1080-F1		30-40	0.29	0.05	0.62	6.0	-4.1	tr.	-5.4	-4.6	0.4	54.0	45.6	7	23	70
	R1148-F1		30-40	0.16	0.03	0.28	6.0	-4.3	-7.1	-5.8	-4.9	n.d.	47.1	52.9	6	32	62
	KM-C1		30-40	0.21	0.04	0.38	6.0	-4.2	tr.	-5.1	-4.5	n.d.	56.0	44.0	6	10	84
	R1097-F2		30-40	0.25	0.04	0.78	5.7	-3.9	-6.8	-6.0	-4.8	n.d.	43.6	56.4	6	53	40
	MD-F1		30-40	0.96	0.06	0.65	6.2	-4.1	tr.	-5.2	-4.2	11.3	53.9	34.8	35	11	55
	R1080-F2		30-40	0.13	0.03	0.15	5.4	-3.8	-7.7	-5.2	-4.2	0.3	38.7	61.0	16	42	43
	RJ-C1		30-40	0.48	0.06	0.68	5.9	-4.2	-7.2	-5.3	-3.9	8.8	61.4	29.8	17	10	73
	MT-C2		30-40	0.09	0.04	0.24	6.4	-3.6	-7.5	-4.8	-4.0	0.9	58.2	40.8	19	10	71
ID-S	JV11	A	0-10	0.47	0.08	0.83	7.7	-3.8	-9.0	-3.8	-3.7	n.d.	42.8	57.2	74	12	14
		R	10-40	0.25	0.07	0.42	6.8	-3.5	tr.	-4.5	-3.7	n.d.	39.8	60.2	—	—	—
	JV17	B1	3-30/35	0.64	0.22	0.96	7.0	-3.5	-8.6	-4.3	-5.3	1.3	78.4	20.3	0	0	100
		B3	60+	0.59	0.23	0.82	7.0	-3.2	tr.	-4.7	-5.6	1.2	73.9	24.9	0	0	100
	EK10	Be	3-20	0.13	0.03	0.28	4.9	-3.5	tr.	-4.5	-3.8	n.d.	49.2	50.8	38	14	48
		Btg	40-55	0.22	0.04	0.24	4.4	-3.5	-6.3	-5.0	-4.2	n.d.	46.9	53.1	34	14	53
	EK11	Be	7-20	0.12	0.05	0.71	7.3	-3.7	tr.	-4.5	-4.3	n.d.	46.5	53.5	—	—	—
		Btg	40-50	0.02	0.04	0.40	6.3	-3.6	tr.	-5.3	-4.8	n.d.	45.6	54.4	50	7	43
	LB41		40-60	0.00	0.03	0.26	4.6	-4.0	-6.3	-5.6	-4.7	2.4	44.8	52.8	57	15	28
	KD01		20-40	0.18	0.02	0.26	4.5	-4.0	-5.9	-5.5	-4.2	n.d.	42.7	57.3	43	17	39
	7		30-60	0.21	0.04	0.35	4.6	-3.9	-6.3	-5.6	-4.7	n.d.	54.5	45.5	43	9	48
	31		30-60	0.13	0.04	0.85	4.6	-3.9	-5.8	-4.0	-4.4	n.d.	54.3	45.7	54	4	43
	14		30-60	0.06	0.03	0.52	4.6	-3.8	-5.9	-5.4	-3.9	n.d.	54.9	45.1	22	12	66
	28		30-60	0.21	0.03	0.11	4.6	-3.9	-6.1	-6.0	-4.4	n.d.	54.1	45.9	41	2	57
	13		30-60	0.00	0.03	0.17	4.3	-3.8	-5.9	-5.4	-4.5	n.d.	63.5	36.5	28	1	71
	SM4	B2t	35-55	0.16	0.05	0.75	4.8	-3.8	tr.	-5.5	-4.5	0.6	49.7	49.7	31	12	57
ID-V	JV1	B	35-63	0.46	0.10	0.78	5.5	-3.7	tr.	-4.5	-5.2	n.d.	52.7	47.3	78	0	22
	JV5	B1	5-45	0.37	0.08	0.68	4.9	-3.8	-6.6	-4.7	-4.1	1.5	83.7	14.7	0	0	100
		B2t	45-60	0.37	0.10	0.54	4.7	-3.9	tr.	-5.3	-4.9	2.2	83.4	14.3	—	—	—
	JV13	B1	6-19	0.36	0.12	0.62	7.5	-3.4	tr.	-3.9	-5.0	n.d.	73.8	26.2	—	—	—
		B2t	19-35	0.00	0.12	0.47	6.2	-3.4	tr.	-4.7	-5.2	n.d.	77.5	22.5	1	0	99
	JV14	A	0-6	0.09	0.06	0.13	8.2	-3.2	tr.	-3.3	-4.4	n.d.	40.4	59.6	93	0	7
		C	6-25	0.12	0.06	0.13	7.1	-3.3	tr.	-5.1	-5.5	n.d.	43.1	56.9	—	—	—
	SM6	BA	2-12	0.12	0.05	0.16	5.8	-3.2	-6.9	-5.0	-3.9	0.2	60.5	39.4	—	—	—
		B2	40-60	0.13	0.03	0.13	5.6	-3.3	tr.	-5.5	-4.3	0.2	62.4	37.4	5	4	91
	SM10	B2t	30-55	0.23	0.03	0.32	5.4	-3.8	-7.0	-6.0	-4.9	1.5	70.8	27.7	20	1	79
	SM13	B	11-30	0.27	0.07	0.89	5.7	-3.5	tr.	-4.9	-4.8	n.d.	69.0	31.0	10	0	90

and a small amount, if any, in TH, ID-S and ID-V. In JP the amount of gibbsite gradually increases with depth in each profile.

According to the contents of Alo, Sio and Feo, most of the samples contain small amounts of amorphous minerals except for KS, SD, AS, JV17 and MD-F1. Judging from the higher contents of Sio, volcanic ash might have been added to SD of JP, JV11 and JV 17 of ID-S and some of ID-V to some degrees.

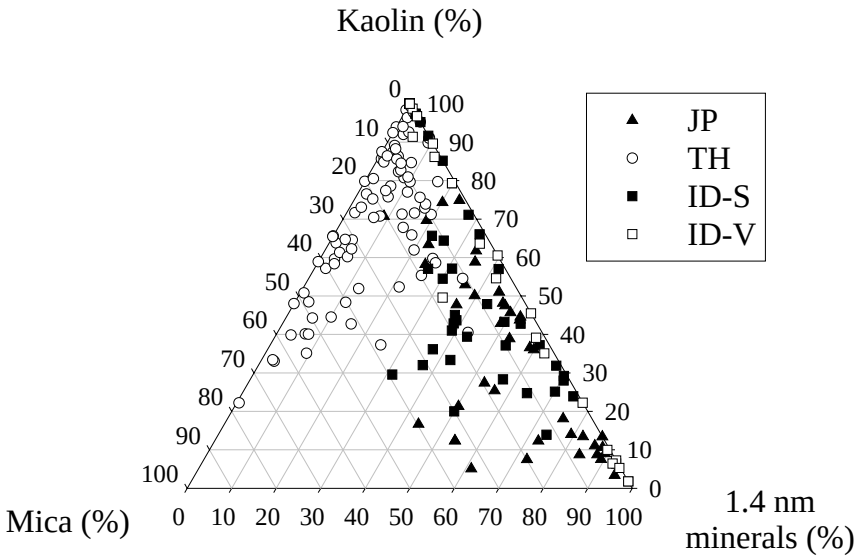

Fig. 2.3. Clay mineralogical composition of the soils determined based on relative peak areas of 0.7, 1.0, and 1.4 nm in X-ray diffractograms.

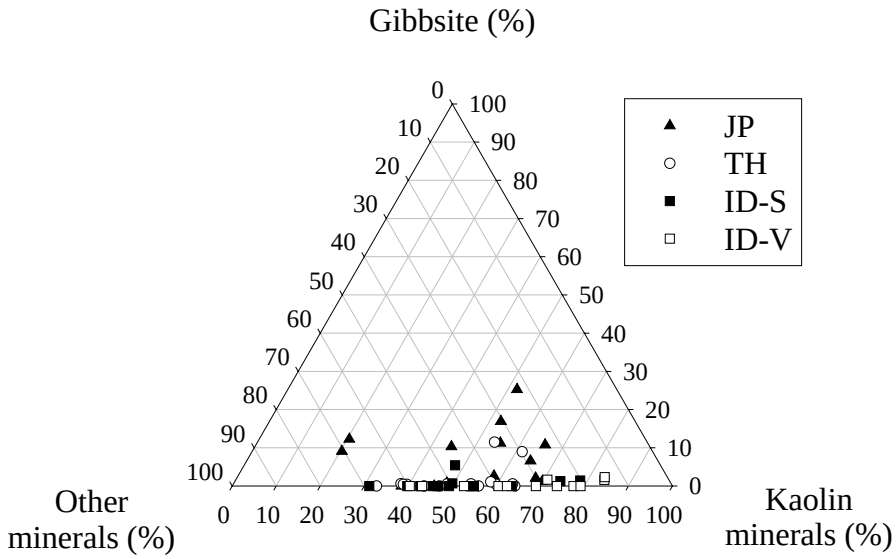

Fig. 2.4. Gibbsite and kaolin contents of the soils determined by thermal analysis.

2.3.2 Chemical composition of quasi-soil-solution

Mineral stability was evaluated for representative samples in each area. Activities of selected cations (Al^{3+}, Mg^{2+}, and K^{+}) of quasi-soil-solution are shown in Table 2.2. The solution compositions are plotted on the stability diagram (Fig. 2.5) and on solubility diagram excluding samples of which Al concentrations are below detection limit (Fig. 2.6). Thermodynamic data used for this study were cited from Karathanasis (2002) for gibbsite, kaolinite, quartz, and amorphous SiO_2 and Lindsay (1979) for amorphous $Al(OH)_3$, muscovite, and microcline.

In JP and ID-S pHs are low as mostly ranging from 4.3 to 5.5, and relatively high in TH and ID-V from 5.4 to 6.5. This result should reflect precipitation and geological condition. In JP and ID-S, high precipitation more than 2000 mm leads to low pH. In TH relatively high pH is attributed to smaller precipitation mostly from 1000 to 1500 mm. In ID-V the pH is still high in spite of high precipitation because the soils contain mafic minerals and/or tephra that

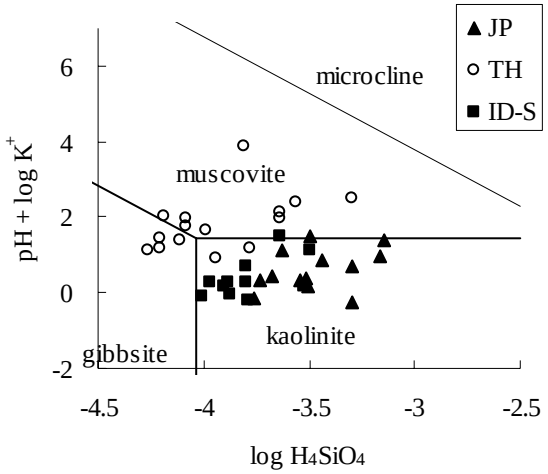

Fig. 2.5. Stability diagram calculated for composition of quasi-soil-solution from JP, TH, and ID-S.

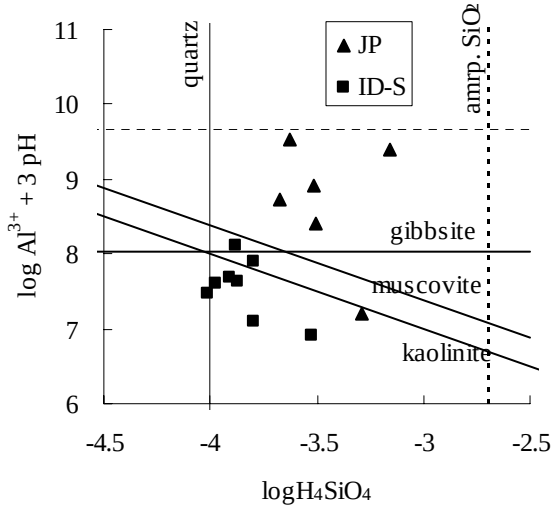

Fig. 2.6. Solubility diagram calculated for composition of quasi-soil-solution from JP and ID-S.

can neutralize acidity through rapid weathering. Generally pHs of quasi-soil-solution are higher than those determined for soil suspension within 1 hour. This fact is explained by gradual dissolution of easily weatherable minerals during 1 week.

In JP, the solutions are characterized by high Al^{3+} and H_4SiO_4 activities in addition to low pH. Most of solution compositions are plotted in kaolinite stable field in the stability diagram (Fig. 2.5). According to the solubility diagram (Fig. 2.6), the solution compositions in JP are between the solubility lines of amorphous $Al(OH)_3$ and gibbsite except for AS, which is plotted below kaolinite solubility line.

In ID-S, pHs are low and most of solution compositions are plotted in kaolinite stable field in stability diagram (Fig. 2.5) as the case of JP. However, in spite of low pH, Al activities are low compared to JP. As pHs decrease, Al activities increase in JP solutions, while the activities do not change in ID-S (Fig. 2.7). In the solubility diagram (Fig. 2.6), the solution compositions are plotted below those of JP, near or under kaolinite solubility line. It implies that the dissolution of kaolinite controls Al activities in ID-S. Activities of H_4SiO_4 also are low in ID-S compared to JP.

In ID-V, high pH and high H_4SiO_4 activity are remarkable (Table 2.2) and the solution compositions are plotted in muscovite stability field in stability diagram except for JV5. In TH, solution compositions are plotted in the field where both kaolinite and muscovite can be stable (Fig. 2.5).

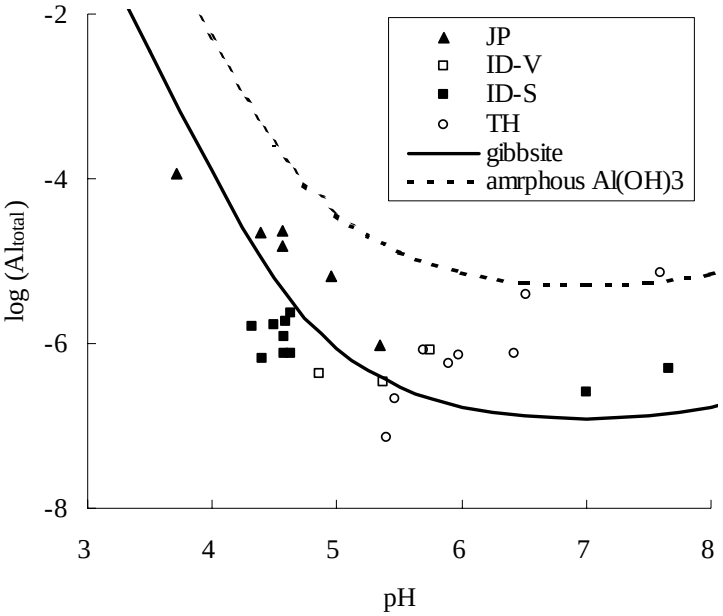

Fig. 2.7. Activity of total Al of the samples with gibbsite and amorphous $Al(OH)_3$ solubility lines. (Al^{3+}), ($AlOH^{2+}$), ($Al(OH)_2^{+}$), ($Al(OH)_3$), and ($Al(OH)_4^{-}$) are included in this calculation.

2.4 Discussion

2.4.1 Si and Al activities

The activities of H_4SiO_4 and Al are very important when considering mineral behavior such as stability, or possibility of neoformation in soil solution. Compositions of quasi-soil-solutions indicate that only small amounts of Si and Al were released from ID-S and TH (Table 2.2).

The H_4SiO_4 activities of quasi-soil-solution are highest in JP ($10^{-3.1}$ to $10^{-3.8}$ mol L^{-1}), then in ID-S ($10^{-3.5}$ to $10^{-4.0}$ mol L^{-1}) and lowest in TH ($10^{-3.6}$ to $10^{-4.3}$ mol L^{-1}). This means that minerals that determine the H_4SiO_4 activity are different. There is no apparent relationship between Sio content of soils and H_4SiO_4 activities of quasi-soil-solution. However, minerals in silt fraction such as feldspars might have little effect on H_4SiO_4 activity in solution because of its small surface area and low dissolution rate (Lasaga 1998). Therefore, though not apparent in the Sio content, the crystallinity of SiO_2 and other clay minerals assumed to determine the H_4SiO_4 activity. The solubility of amorphous SiO_2 is reported to be $10^{-2.7}$ mol L^{-1} and that of quartz 10^{-4} mol L^{-1} (Karathanasis 2002). In the soils the crystallinity of SiO_2 is between the two. Lindsay (1979) presents the solubility of soil SiO_2 as $10^{-3.1}$ mol L^{-1}. Considering the fact that H_4SiO_4 activity is much lower in tropical areas except for ID-V, which contains volcanic ash, than in temperate zone, crystallinity of clay minerals is higher in the former. In addition, in TH, low dissolution rate of minerals under higher pH range (mostly 5.7 – 6.5) might be another reason for low H_4SiO_4 activity.

Similar reason may be applicable for the case of Al activity. In JP amorphous $Al(OH)_3$ (or other minerals with low crystallinity, such as pedogenetic kaolin) thought to be main sources of solution Al. In ID-S, judging from the fact that its solution composition is near kaolinite solubility line, the low Al activity is considered to be controlled by kaolinite dissolution. In TH, pHs are high and thus it is difficult to detect solution Al in most samples. The source of Al of the samples of TH can be primary minerals in silt fraction such as feldspars, because the solution compositions are plotted above those of JP and ID-S and total Al released in TH solutions are less than $10^{-6.0}$ mol L^{-1}, which means that a very small amount of the mineral dissolution is required for Al supply in this range.

2.4.2 Transformation of 2:1 type clay minerals

In the case of TH, mica is relatively stable and not transform to 1.4 nm minerals so easily, while other primary minerals such as feldspars are unstable and dissolve to form kaolinite. Araki et al. (1998) investigated weathering of Tanzanian soils, at which the presence of a distinct dry season is somewhat similar to Thailand, and reported weathering process of mica

without forming 1.4 nm minerals. They assume that it takes very long time (perhaps several million years) for mica to weather to kaolinite and/or gibbsite. According to the stability diagram, both the pH and K^+ activity in solution are important for mica weathering, i.e., kaolinite is getting more stable than mica as pH and/or K activity decreases (Fig. 2.5). For example, the work of Rausell-Colom et al. (1965) indicates that the removal of K from micas is strongly dependent on the K concentration of the solution. In our experiment, however, there is no evidence of K depletion in the solution of JP and ID-S, because the K^+ activity ranges from $10^{-3.8}$ to $10^{-4.8}$ mol L^{-1} and almost same as that of TH. This implies pH plays an important role in *in situ* mica weathering. In this study, an apparent border of pH(H_2O) for mica weathering to 1.4 nm minerals is between 5.5 and 5.0, above which mica can weather directly to kaolinite without forming 1.4 nm minerals.

In JP, quasi-soil-solutions are plotted in the kaolinite stable field. This is interpreted as that mica inherited from parent minerals dissolve to form kaolinite and in this process 1.4 nm minerals such as HIV and vermiculite form as transitional products. Low crystalline clay minerals and perhaps easily weatherable primary minerals dissolve and release Al to the soil solution. The released Al may precipitate as Al hydroxides between 2:1 layers. The 2:1 layers of HIV seems to be stable, probably because of buffering capacity of interlayered materials that can react with further acid load more easily than the 2:1 layers. Such a preferential dissolution of interlayered materials in 2:1 layers is widely observed in surface horizons of acidic soils e.g., podzolic soils (Hirai et al. 1991; Funakawa et al. 1992). This may be why vermiculite is predominant in upper or more acidified horizons.

In ID-S there are mica minerals found in parent rocks and they also weather to form vermiculite and smectite. It is considered that a small amount of easily weatherable minerals are present in these soils, if any, under tropical rainforest climate and in turn a potential for acid neutralization through mineral dissolution is limited. As a result, interlayered materials may have already dissolved and vermiculite and/or smectite form as indicated in Fig. 2.2.

2.4.3 Neoformation of kaolinite, smectite, and gibbsite

Kaolin minerals are observed in all the samples, implying that the forming conditions of kaolin minerals are very common. In acid soils such as ID-S and AS of JP, kaolinite may dissolve judging from the solution composition on the solubility diagram.

In some samples of which parent materials do not contain mica, smectite can precipitate from soil solution at the initial stage of mineral weathering under high H_4SiO_4 activity. It is often reported that in the solution of high pH and high Si and Mg activities, smectite forms (Reid-Soukup and Uley 2002). Such conditions are likely to meet for some soils derived from mafic materials, most of ID-V in this study.

Distribution of gibbsite in Inceptisols and Ultisols are widely reported (Cook 1973; Iwasa

1977;Nortfleet et al. 1993; Cleavert et al. 1980a,b; Rbertus and Buol 1985; Rbertus et al. 1986; Araki 1993; Ogg and Baker 1999), and in most cases gibbsite decreases from lower to upper horizons. Iwasa (1977) investigated clay mineral composition of soils derived from granite in different bio-climatic zones, i.e., temperate to humid torrid regions and reported that there are large amount of gibbsite in temperate zone and very small amount in tropical and subtropical zones. In our study, gibbsite forms in all of the JP soils with a decreasing trend toward the soil surfaces, while in the other regions a small amount of gibbsite forms, if any. Judging form the total Al activity and pH of the quasi-solution (Fig. 2.7), gibbsite can form in solutions because solution composition is supersaturated with gibbsite, except for ID-S samples. Nortfleet et al. (1993) indicate the formation of gibbsite in weathering saprolites, where H_4SiO_4 activity seemed to be enough high for formation of alminosillicate, are due to rapid removal of water and Si from intensive weathering zones, or to local environment where H_4SiO_4 activity is low. There is another possibility for gibbsite formation in solution where H_4SiO_4 activity is high, that it precipitates much more easily and rapidly than kaolin. Further, poorly ordered Al may help to form gibbsite, though up to present this phenomenon observed only in laboratory (Huang et al. 2002). Cleavert et al. (1980a,b) and Furian et al. (2002) report the resillication of gibbsite in North Carolina, America and southeastern Brazil. Considering these reports and possibilities together with geological and weathering conditions of Japan, presumably gibbsite forms together with amorphous Al and Si and low crystalline kaolin in early stage of weathering as unstable transitional minerals. Then it resillicates to form stable mineral or kaolinite, which precipitate slowly under moderate H_4SiO_4 activities. Coexistence of gibbsite and smectite, the latter of which is stable only under high Si activities, in KS may supports the possibility of temporal presence of gibbsite. Antigibbsite effect (Jackson 1963) was not apparent in this study. Rather gibbsite decreases along with decrease of interlayed materials toward the soil surfaces, probably because of acidification or resillication. Considering solution compositions (Fig. 2.7), in some of TH, JV17 of ID-S and some of ID-V, gibbsite may form in initial weathering stage. Moreover, in TH the very low H_4SiO_4 activities also could be responsible for gibbsite formation and stability, though the amount of gibbsite and H_4SiO_4 activity has no apparent correlation. In contrast, gibbsite was not formed in ID-S or already disappeared, if any, except for LB41, because gibbsite dissolve much faster than kaolinite under low pH and low Al activity (Lasaga 1998). In LB41, judging from broader peak at 0.7 nm in X-ray diffractogram, the crystallinity of kaolinite is lower than the other samples of ID-S, which means LB41 is relatively young and still contains gibbsite.

Chapter 3
Cs adsorption and desorption on soils with different mineralogical composition

3.1 General

As mentioned in Chapter 1, small mobility of Cs^+ in soil environment is primarily caused by specific adsorption onto clay minerals. Clay minerals, particularly 2:1 phyllosilicates, play the most important role in the Cs immobilization. Even soils with high in organic matter content, the clay fraction, however small it may be, is responsible for the Cs immobilization (Hird et al., 1995).

Of all the 2:1 phyllosilicate illite and vermiculite are mainly responsible for the Cs immobilization (Klobe et al., 1970; Maes et al., 1999a,b; Seaman et al., 2001). The mechanism of Cs immobilization on illite can be explained by Cs-K exchange on the frayed edge site (FES) that is formed by the juxtaposition of a non-expandable and an expandable (i.e. hydrated) interlayer. The mechanism can be separated into four steps: 1) opening of the interlaer spacing (delamination), 2) hydration and release of interlayer K, 3) sorption and dehydration of Cs, and 4) closing of interlayer spacing (Rosso, 2001). Springob (1999) reported that the Cs adsorption on FES regulates the K^+ release from interlayers of illitic clays. On the other hand, the mechanism of Cs immobilization on vermiculite can be explained by collapse of hydrated interlayers which can occur followed by Cs immobilization on FES. Hird et al. (1996) showed that the interlayer collapsed and Cs^+ is subsequently immobilized when the concentration of Cs^+ in the vicinity of wedge zones amounted to about >0.75 mM.

High charge smectite also immobilize Cs^+ though its charge density is less than that of vermiculite. This is caused by the adsorption on the interlayers with tetrahedral isomorphic substitutions. The 2:1 layer structure consists of two tetrahedral sheets with one bound to each side of an octahedral sheet. Isomorphic cationic substitutions can occur either in the octahedral or in the tetrahedral sheet of 2:1 phyllosilicates, and the negative charge by the isomorphic substitution in the tetrahedral sheet adsorb metal cations more strongly because of the close proximity to the cations. If the adsorbed cation is easily dehydrated monovalent cation such as K^+, NH_4^+, Rb^+, and Cs^+, the adsorption on the tetrahedral charged site result in the immobilization of them.

Borchardt (1989) reported that when the immobilization does occur in smectitic soils or minerals, it is often due to the inclusion of other minerals, such as vermiculite or weathered mica, or the presence of wedge zones in the smectite mineral. However, Maes et al. (1999a) reported that ‘degradation smectite’ (i.e. smectite-like minerals that present a 1.7-1.8 nm reflection in their X-ray diffraction after saturation with Mg^{2+} and etylen-glycol solvation, but collapse to 1.0 nm when heated (200ºC) after saturation with K^+) dominates the Cs

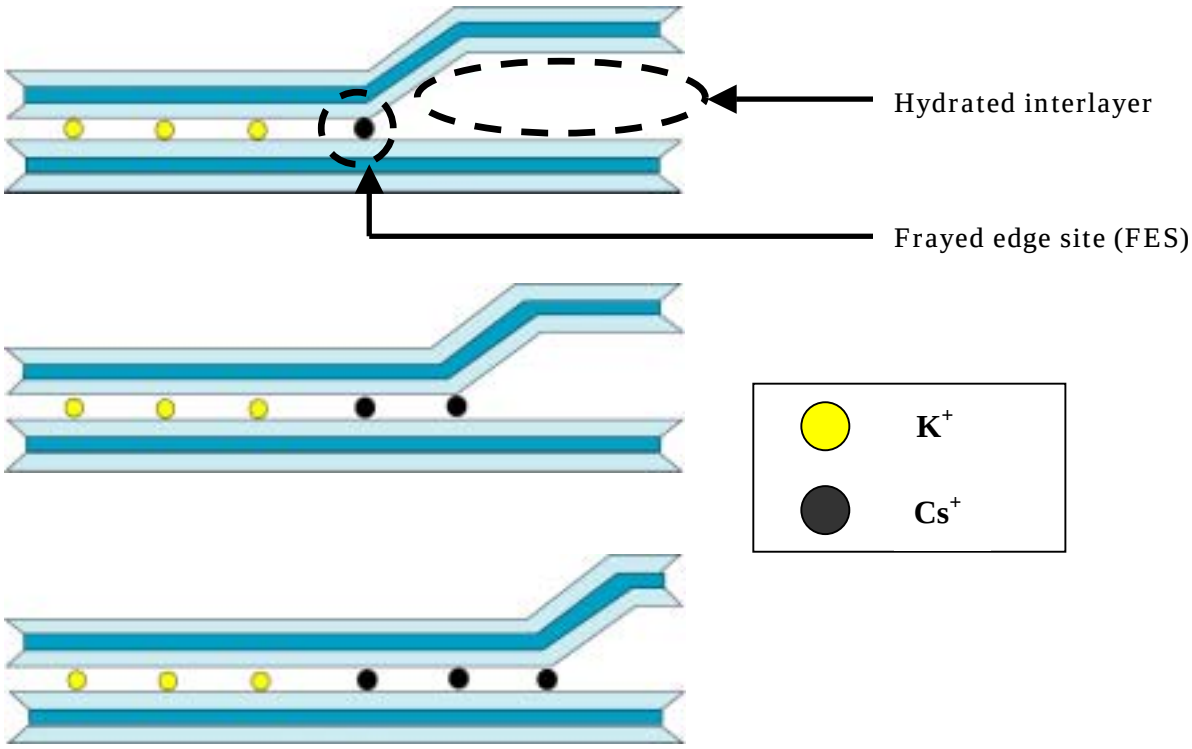

Fig. 3.1. The schematic illustration of the collapsing process of the interlayer sites of 2:1 phyllosilicates along with increasing Cs^+ saturation of interlayer sites. The collapse may not occur if the interlayer sites have no tetrahedral isomorphic substitutions.

immobilization capacity though it's weaker than that of illite or vermiculite.

Thus it is FES and interlayers with tetrahedral isomorphic substitutions that responsible for Cs immobilization. However the Cs immobilization on collapsed interlayers does not occur if the Cs^+ concentration of a soil solution is below 0.75 mM.

The above is what early studies have shown about Cs immobilizing mechanisms. These mechanisms are, however, usually studied at the equilibrium conditions. We have to understand time dependent mechanisms of Cs immobilization in addition to such a classical approach.

3.2 Materials and methods

3.2.1 Soil samples

Totally 20 surface soils were collected from Ukraine (UA), Japan (JP), Indonesia (ID), and Thailand (TH). UA soils were mainly collected from northern part of Ukraine near

Table 3.1. Number of soil samples with reference to land use and parent materials. Parenthesis denotes subsurface samples.

	Land use	Parent materials				
		Loess	Sedimentary rock	Granite	Andesite	Limestone
Ukraine (UA)	Cropland	3				
	Forest	2 (1)				
	Grassland	2				
Japan (JP)	Cropland		1			1
	Forest		2 (1)			
Indonesia (ID)	Cropland		2		1	1
Thai (TH)	Cropland		2 (1)	1		

Chernobyl. The number of samples with reference to land uses and parent materials are listed in Table 3.1. Parent material of UA samples is loess while those of the other areas are variable. The annual temperature and precipitation of northern Ukraine are about 8ºC and 600 mm, respectively. On the other hand, the annual temperature of Japan, Indonesia and Thailand are higher than that of Ukraine, i.e., 10-20ºC in Japan, 20-25ºC in Thailand, and above 25ºC in Indonesia, respectively. The annual precipitation in Japan, Indonesia, and Thailand is also much higher (usually greater than 1000 mm) than in Ukraine. Generally speaking, the UA soils are less weathered than the others. All the soils used in this study contain a fairly large amount of 2:1 phyllosilicates.

3.2.2 Clay mineralogical composition of the soils

The mineralogical compositions of clay fraction were determined by X-ray diffraction (XRD) using an oriented clay specimen with Mg^{2+} or K^{+} saturation, and glycerol solvation followed by Mg^{2+} saturation. Figure 3.2 illustrates typical XRD patterns expected for ideal clay specimen. The soil samples were classified into three groups based on dominant 2:1 clay mineral species, that is, 1) expandable clay minerals with octahedral isomorphic substitution (OE), 2) expandable clay minerals predominantly with tetrahedral isomorphic substitutions (TE), and 3) non-expandable clay minerals (NE), according to Fig. 3.3, briefly described below.

1) Samples that do not exhibit any peaks derived from 2:1 minerals (i.e., 1.0 and 1.4 nm peaks) after Mg saturation are excluded from this analysis.
2) Samples that exhibit only 1.0 nm peak without 1.4 nm peak after Mg saturation are considered to be dominated by mica minerals and classified into the category, NE.

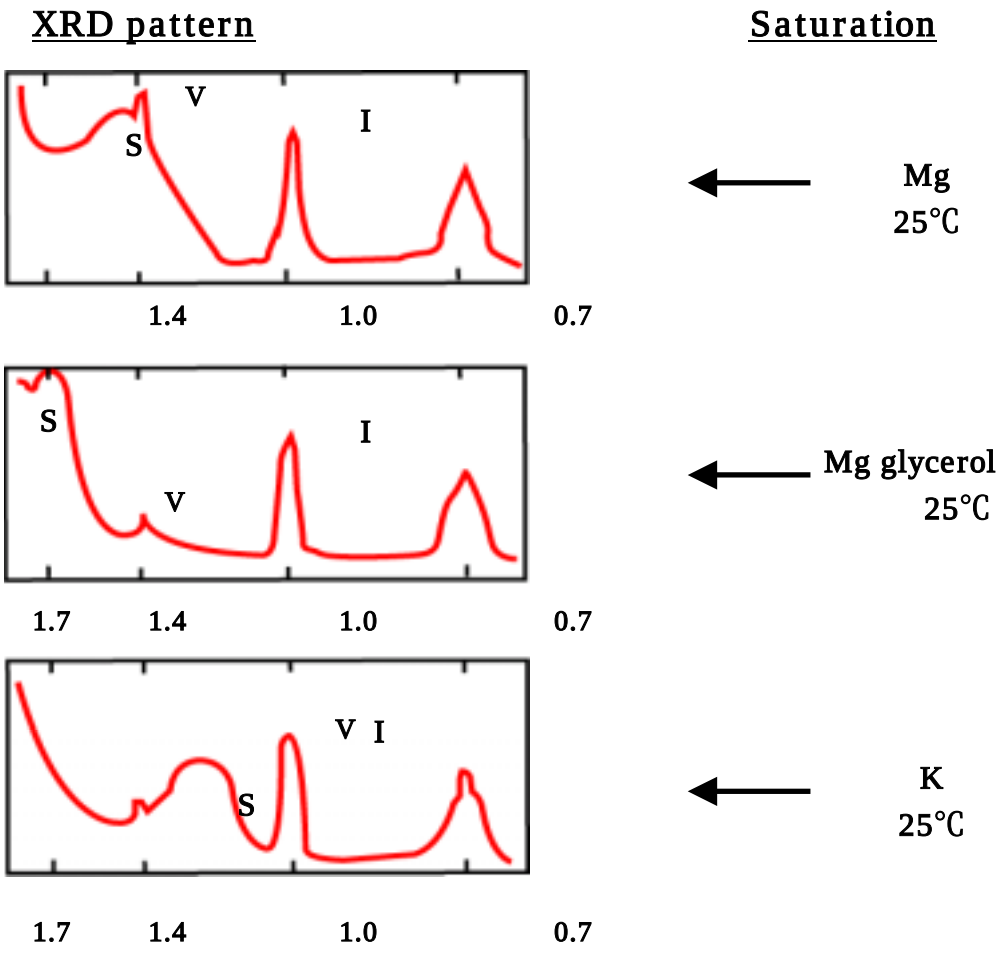

Fig. 3.2. Representative patterns of X-ray diffractograms for ideal clay specimen containing smectite (S), vermiculite (V), illite (I), and kaolinite (K).

3) Samples that exhibit a 1.4 nm peak with or without a 1.0 nm peak after Mg saturation would contain a certain amount of expandable 2:1 minerals. These soils are further analyzed to specify which 2:1 minerals are dominant, based on peak shifts both after glycerol solvation of Mg-saturated specimen and K-saturation treatment as below.

i) Samples, of which 1.4 nm peak expands to 1.5 to 1.8 nm after glycerol solvation, are judged to contain a fairly large amount of smectites and further tested by K-saturated specimen.

a) If the 1.4 nm peak of the sample collapse to 1.2 to 1.4 nm in K-saturated specimen, the main component is considered to be smectites with a relatively low charge density. These samples are regarded to be dominated by octahedral isomorphic substitution and classified into the category, OE.

b) If the 1.4 nm peak collapsed to 1.0 nm in K-saturated specimen, the main component is considered to be smectites with a relatively high charge density. These samples might be dominated by tetrahedral isomorphic substitution and

classified into the category, TE.

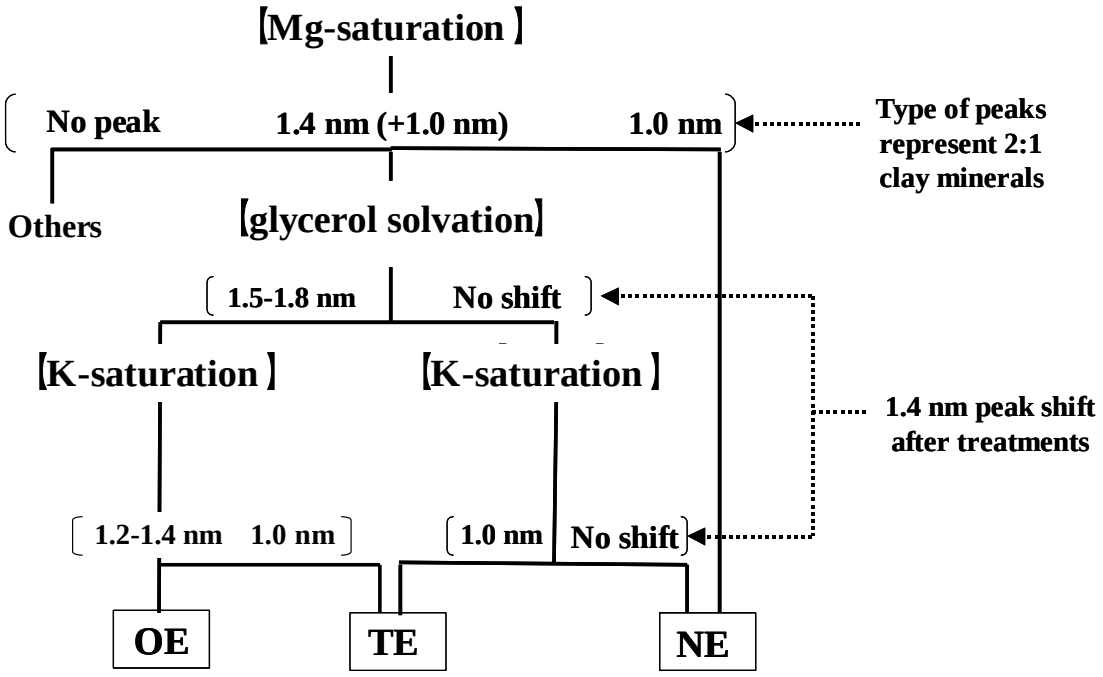

Fig. 3.3. Schematic chart for soil classification based on the mineralogical composition.
【 】represents the type of ion saturation and treatment.

ii) Samples, of which 1.4 nm peak do not shift after glycerol solvation, are considered to be vermiculites-dominant with a certain amount of tetrahedral isomorphic substitution and further tested by K-saturated specimen.

a) If the 1.4 nm peak of the sample collapse to 1.0 nm after K saturation, the main component is considered to be vermiculites and classified into the category, TE.

b) If the 1.4 nm peak does not shift after K-saturation, the main components are hydroxy-interlayered vermiculite (HIV). In this case, the interlayer spaces are already occupied by Al hysroxides and/or Al-Si complexes. Therefore they are classified into the category, NE.

3.2.3 Cs adsorption and desorption with batch method

Soil samples were saturated with $CaCl_2$ or CsCl as preparation for the Cs adsorption or desorption experiment. Air-dried soil was sieved through 0.02 mm mash and 0.5 g of the sieved sample was weighed into 50 mL centrifuge tube. Then the sample was shaken for 30 min together with 40 mL of 1 M $CaCl_2$ and then centrifuged by 2000 rpm for 10 min to separate the supernatant solution, which was then discarded. This saturation procedure with 1 M $CaCl_2$ was repeated again. The soil was washed twice with 40 mL of 0.01 M $CaCl_2$ and then twice with 10 mL of 80 % ethanol to reduce the concentration of entrained Ca^{2+}. Then

the soil sample was dried for 12 hr at 60ºC and served for the next Cs-adsorption procedure. Preparation of Cs-saturated sample traces the same procedure as Ca-saturation, but 0.5 M CsCl and 0.01 M CsCl were used for saturation treatment instead of $CaCl_2$ solutions.

The Cs adsorption experiment was conducted following the Ca saturation procedure. The dried sample in the centrifuge tube was mixed with 40 mL of 10 mM CsCl solution. After shaking for 60 min, the suspension was centrifuged by 2500 rpm for 10 min to separate a supernatant, which was then filtrated and collected. The concentration of Ca^{2+} extracted from Ca-saturated sample was measured by atomic absorption spectrophotometry (AAS). Here the concentration of Ca^{2+} extracted by CsCl solution was assumed to be equivalent to adsorbed Cs^{+}.

For Cs desorption experiment, the Cs-saturated soil sample was mixed with 40 mL of 10 mM $CaCl_2$ solution following the Ca saturation procedure. The suspension was shaken for 60 min and centrifuged by 2500 rpm in 10 min to separate a supernatant, which was then filtrated and collected. The concentration of Cs^{+} extracted from Cs-saturated sample was measured by AAS.

3.2.4 Cs adsorption and desorption with continuous flow method

Samples were saturated with $CaCl_2$ or CsCl as preparation for the Cs adsorption or desorption experiment. A 5g of sieved soil sample (<0.02 mm) were weighed into 50 mL centrifuge tube and shaken for 30 min with 40 mL of 1 M $CaCl_2$. Then the suspension was centrifuged by 2000 rpm for 10 min in order to separate supernatant solution, which was then discarded. This saturation procedure with 1 M $CaCl_2$ was repeated again. The sample was then washed twice with 40 mL of 0.01 M $CaCl_2$ and transferred into a dialysis bag, which was soaked in distilled water to reduce the concentration of entrained Ca^{2+}. The distilled water was renewed once in a day until the EC value decreased to 1-4 $\mu S\ cm^{-1}$. The Ca-saturated soil was then freeze-dried. The preparation of Cs-saturated samples traces the same procedure as Ca-saturation, but 0.5 M CsCl and 0.01 M CsCl were used for saturation treatment instead of $CaCl_2$ solutions.

On column setting, the soil sample prepared was diluted by quartz sand to adjust the clay content and CEC to 15 % and 30 μmolc, respectively, in order to eliminate a possible variation derived from difference in volume for ion exchange reactions. The adjusted sample was then put into a glass column with embedded between two 0.2 g of inert quartz sands and both inlet and outlet part of the glass column were filled with quartz cottons to prevent loss of clay particles through dispersion (Fig. 3.4).

For Cs adsorption, 0.75 or 7.5 mM CsCl solutions was used as a influent while 0.2 or 2.0 mM $CaCl_2$ solution was used for Cs desorption. Here the concentrations of CsCl and $CaCl_2$ solutions were selected based on the facts that the interlayer collapses usually occur in a Cs

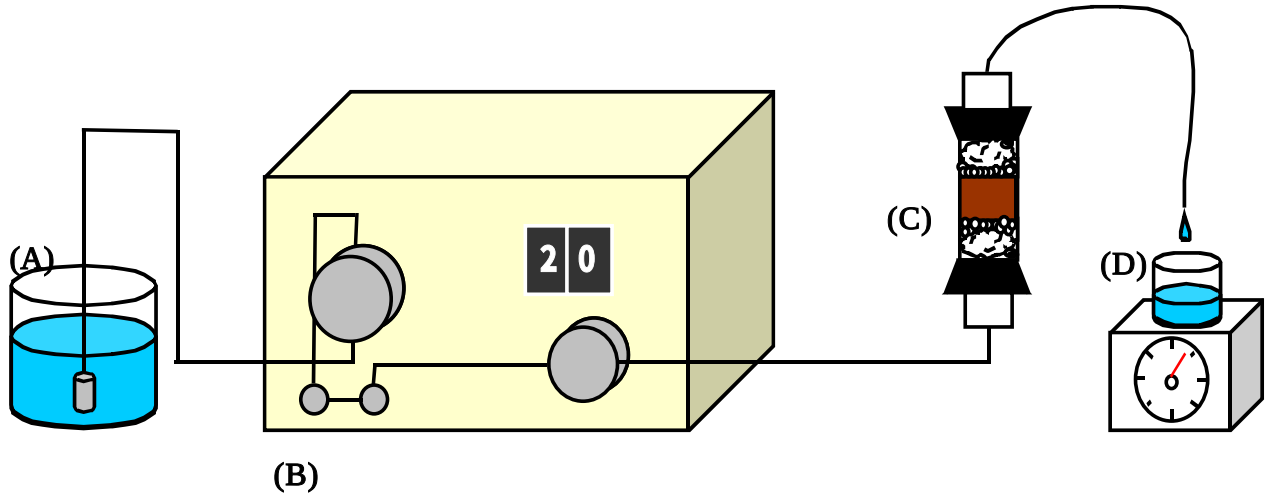

Fig. 3.4. Diagram of the instrument that was used for the continuous flow method.

(A) Influent solution: Concentrations are adjusted to 0.75 or 7.5 mmol L^{-1} CsCl for Cs adsorption experiment or to 0.2 or 2.0 mmol L^{-1} $CaCl_2$ for Cs desorption experiment. Solution pH is always adjusted to 5.

(B) Peristaltic pump: The flow rate is kept constant (2.0 mL min^{-1}).

(C) Soil in a glass column: Clay content and cation exchange capacity are adjusted to 15% and 30 μm by dilution with fine quartz sands. They are embedded with coarse quartz sands and quartz cotton to prevent loss of dispersed clay particles.

(D) Effluent solution: It is collected every ten minutes. Then concentrations of Cs^+ and Ca^{2+} of each aliquot was measured by AAS.

concentration range, between 0.60 and 0.75 mM (Hird et al., 1996). The relationship between ionic strength (I) and concentration of individual ions in solution is expressed as:

$$I = 1/2 \sum Z_i^2 * c_i \qquad (1)$$

where Z_i is the valence and c_i is the concentration of ion i in mol L^{-1}. Thus the ion strength of 0.2 mM $CaCl_2$ solution is close to that of 0.75 mM CsCl solution.

The pH of each solution was adjusted to 5, and the influent solution was pumped into the glass column at a constant rate of 2.0 mL min^{-1} (Fig. 3.4). The experiment was conducted for 60 min at a constant temperature (25ºC) and the effluent solutions were collected every 10 min. Both the Cs^+ and Ca^{2+} concentrations of each aliquot were measured by AAS after 10 times dilution. The datasets obtained were simulated using the first order kinetic model:

$$y = a\,(1\text{-}exp(\text{-}kt)) \qquad (2)$$

where a is the adsorption (or desorption) maximum in mg kg^{-1} and k the rate constant in min^{-1}.

3.3 Result and Discussion

3.3.1 Soil properties and mineralogical classification

Table 3.2 represents physicochemical properties of the soil samples used for the batch experiment. All of the soils were collected from surface layers except for JP-f1 and JP-f2, which were collected from subsurface horizon (9-15 cm) in order to eliminate a possibly high contribution of organic matter (i.e. 202 and 244 g kg^{-1} C in JP-f1 and JP-f2, respectively). The values of pH of UA soils were rather similar each other as ranging from 5.2 to 5.9, suggesting relatively homogeneous conditions in parent materials and climates. On the contrary, most of the soils from JP and ID were acidic, reflecting humid climatic conditions there (except for the samples whose parent material is limestone (JP-c2 and ID-c1)). The pH values of TH soils were generally higher than those of JP or ID soils presumably because of lower annual precipitation in Thailand (1000-2000 mm).

Table 3.2. Physicochemical properties of soil samples for batch experiment.

Uk: Ukraine, Jp: Japan, In: Indonesia, Th: Thailand; f: forest, c: cropland, g: grassland.

Site	Sand (%)	Silt (%)	Clay (%)	pH H_2O (1:5)	Total C (g kg^{-1})	CEC ($cmol_c$ kg^{-1})	Group
UA-f1	32.5	36.9	30.5	5.2	27	18.4	OE
UA-f2	46.1	27.6	26.3	5.6	26	22.7	〃
UA-c1	54.4	20.7	24.9	5.8	27	28.8	〃
UA-c2	67.8	17.5	14.6	5.6	7	6.5	〃
UA-c3	49.4	23.9	26.7	5.9	24	21.2	〃
UA-g1	84.5	8.9	6.6	5.4	8	4.8	〃
UA-g2	77.7	13.2	9.1	5.7	6	5.8	〃
JP-f1	40.3	30.5	29.2	3.7	26	17.9	TE
JP-f3	27.1	39.9	33.0	3.8	29	17.8	〃
JP-c1	13.9	38.0	48.1	4.8	44	30.7	OE
JP-c2	15.9	40.7	43.5	8.4	11	26.4	TE
JP-c3	41.7	27.4	30.9	5.7	41	22.9	〃
JP-c4	9.5	42.5	48.0	6.5	13	17.5	〃
ID-c1	82.2	12.7	5.1	6.5	17	26.1	OE
ID-c2	12.7	22.2	65.2	4.2	25	45.4	〃
ID-c3	16.7	16.0	67.3	4.4	22	19.3	〃
ID-c4	45.8	25.5	28.7	4.1	12	12.8	TE
TH-c1	63.6	10.5	25.9	6.1	15	6.7	NE
TH-c2	36.2	22.4	41.3	7.2	30	16.6	〃
TH-c3	8.5	23.9	67.6	5.3	47	n.d.	〃

Figure 3.5 shows representative X-ray diffractograms of clay specimen from the soils studied. Figure 3.5(a) represents X-ray diffractograms of UA-f2 and most of the UA soils showed this pattern. Figure 3.5(b) represents X-ray diffractograms of ID-c1. JP-c1, ID-c1, ID-c2, and ID-c3 showed this pattern. In these cases, the 1.4 nm peak in Mg-saturated specimen expanded to 1.7 nm or greater after glycerol solvation and exhibited an incomplete collapse to around 1.2 nm in K-saturated specimen. Thus they can be classified into OE group based on the classification that described above.

Figure 3.5(c) represents X-ray diffractograms of JP-f1. JP-f2, JP-c2, and ID-c4 showed similar patterns. In these diffractograms, the 1.4 nm peak of Mg-saturated specimen partially shifted to 1.7 nm after glycerol solvation and collapsed to 1.0 nm almost completely in the K-saturated specimen. Vermiculites and high-charge smectites may coexist in this sample. The extents of expansion of 1.4 nm peak after glycerol solvation are variable among the soils. Figure 3.5(d) represents X-ray diffractograms of JP-c4. JP-c3 also showed a similar pattern. The 1.4 nm peak in Mg-saturated specimen did not expand after glycerol solvation and, on the other hand, collapsed to 1.0 nm to some degree in K-saturated specimen. Vermiculites and hydroxy-interlayered vermiculite (HIV) may coexist in this soil. They can be classified into TE group.

Figure 3.5(e) represents X-ray diffractograms of TH-c1. The XRD pattern of Mg-saturated specimen did not show apparent 1.4 nm peak, which indicates that the sample contains apparently no expandable 2:1 phyllosilicates. The TH soils (TH-c2 and TH-c3) exhibited similar XRD pattern to Fig. 3.5(e). It means that these samples are dominated by mica minerals among 2:1 minerals and did not contain appreciable amounts of expandable 2:1 phyllosilicates. They can be classified into NE group.

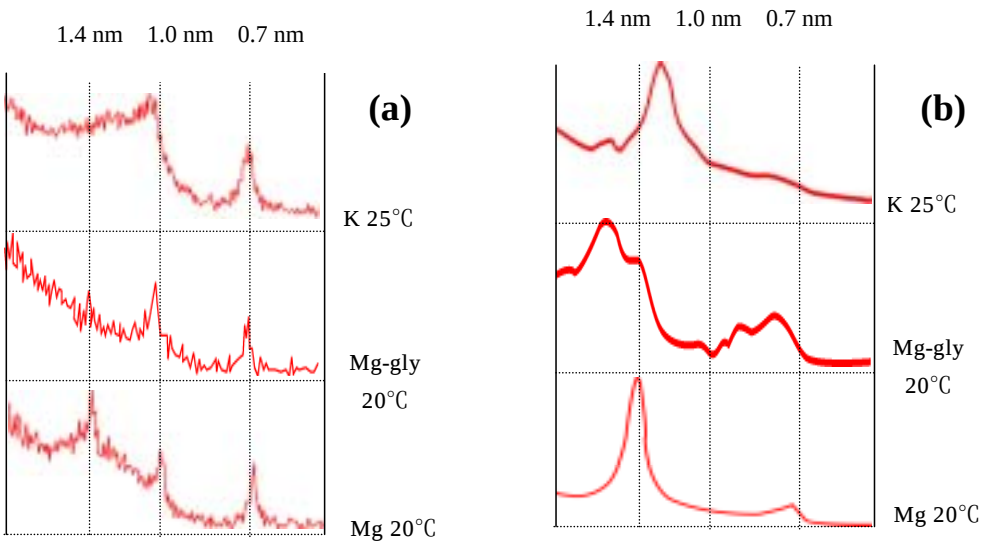

Fig. 3.5. X-ray diffractgrams of clay samples from representative soils.

(a) UA-f2, (b) ID-c1, (c) JP-f1, (d) JP-c4, (e) TH-c1;

Mg 25°C: saturated with Mg and air-dried at room temperature, Mg-gly 25°C: saturated with Mg followed by glycerol solvation, K 25°C: saturated with K and air-dried at room temperature.

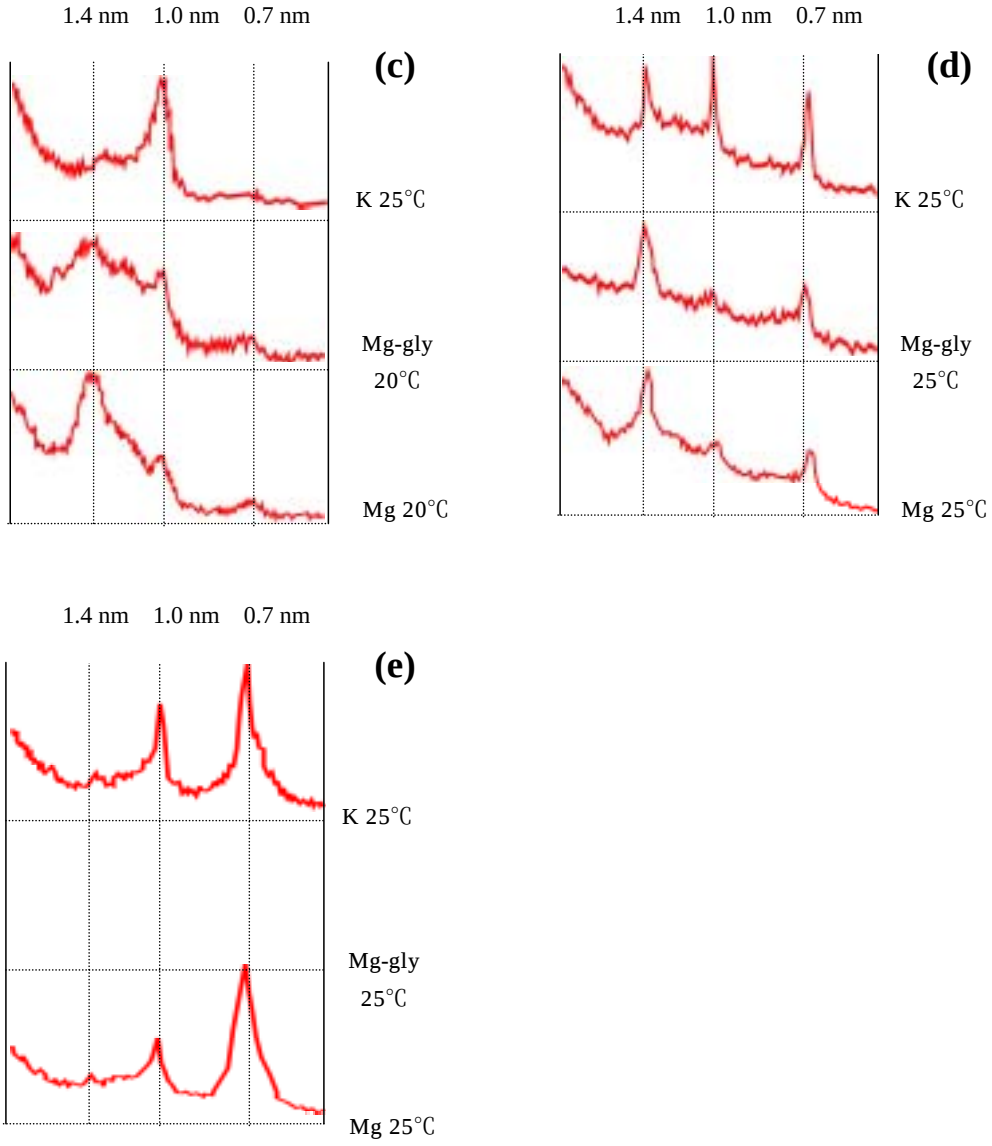

3.3.2 Cs adsorption and desorption for batch method

The Cs adsorption and desorption data for each soil sample are presented in Table 3.2 and Fig. 3.6. In OE group, desorption ratio of the UA soils (0.7-1.2) were relatively higher than the other OE soils (0.3-0.7). These two types can be differentiated based on the XRD patterns. The XRD patterns of the UA soils corresponded to Fig. 3.5(a) and that of the other OE soils to Fig. 3.5(b). In the former the 1.4 nm peak observed in Mg-saturated specimen almost disappeared after glycerol solvation, presumably because more than two molecule layers of glycerol could enter into the interlayer space of smectites due to a lower charge density in each 2:1 layer than the latter smectites, in which exactly two molecule layers of glycerol were retained. Such a difference in charge density of 2:1 layers may explain the difference of smectites in the UA soils and that in the others in terms of Cs immobilization.

As mentioned above, the UA soils did not exhibit XRD pattern containing smectites with tetrahedral isomorphic substitution, but it was not clear whether 2:1 octatrahedral or FES may contribute to Cs immobilization. Figure 3.7 represents a relationship between cation exchange capacities CEC per clay (CEC/clay) and the desorption ratio. The value of CEC/clay was strongly correlated with desorption ratio (r = 0.96) whereas CEC/total C content was not correlated (r = 0.18), indicating that the desorption ratio is getting higher with increase in CEC/clay. That is, the larger amount of CEC per clay they have, the smalleramount of Cs soils can be immobilized. Normally expandable 2:1 phyllosilicates contribute to larger amount of CEC than any other clay minerals. Therefore smaller CEC/clay means a larger inclusion of other minerals. In the case of UA soils, a smaller desorption ratio (a larger immobilization) is considered to be caused by a larger inclusion of FES of weathered mica. Thus it should be not the 2:1 phyllosilicates with octahedral isomorphic substitution but the FES that determine the Cs immobilizing capacity of the UA soils.

The samples of the TE group showed various desorption ratios ranging from 0.3 to 1.1, but the TE soils can be classified subsequently into two groups whether the soils contain HIV or not. The TE soils containing HIV showed high desorption ratios of around 1 whereas the TE soils that do not contain HIV exhibited relatively low desorption ratios (0.3-0.5). It may be because that interlayered compounds block the access of Cs^+ ion to the immobilizing sites through neutralizing layer charge or physical interference. This result suggests that 2:1 phyllosilicates with tetrahedral isomorphic subustitutions potentially have a large capacity for immobilizing Cs^+ unless hydroxy-interlayering is not appreciable.

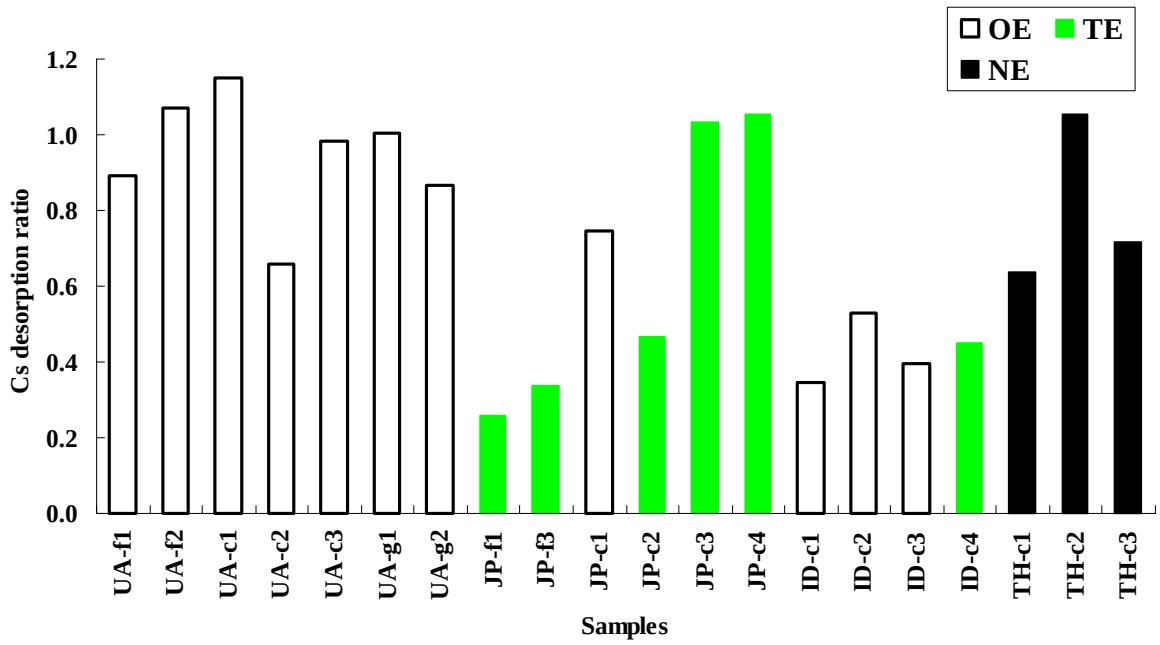

Fig. 3.6. Cs desorption ratio of 20 samples determined in the batch experiment.

The NE soils showed relatively higher Cs desorption ratios. Since they do not contain expandable 2:1 phyllosilicates that can immobilize Cs^+, it should be FESs in mica minerals are considered to be main components that immobilize Cs^+.

Thus we conclude that vermiculites and high-charge smectites having tetrahedral isomorphic substitutions immobilize a large amount of Cs^+ unless hydroxy-interlayering is not appreciable, as well as FES of weathered mica.

Table 3.3. Amounts of adsorbed and desorbed Cs ($cmol_c\ kg^{-1}$), desorption ratio (desorbed Cs / adsorbed Cs), and grouping of each sample.

Sample	Group	Cs adsorbed ($cmol_c\ kg^{-2}$)	Cs desorbed ($cmol_c\ kg^{-3}$)	Desorption Ratio
UA-f1	OE	11.5	10.3	0.9
UA-f2	〃	11.1	11.9	1.1
UA-c1	〃	10.8	12.5	1.2
UA-c2	〃	5.0	3.3	0.7
UA-c3	〃	11.5	11.4	1.0
UA-g1	〃	2.5	2.5	1.0
UA-g2	〃	3.3	2.9	0.9
JP-f1	TE	14.3	3.7	0.3
JP-f3	〃	11.3	3.8	0.3
JP-c1	OE	12.5	9.3	0.7
JP-c2	TE	22.9	10.7	0.5
JP-c3	〃	6.5	6.7	1.0
JP-c4	〃	8.4	8.8	1.1
ID-c1	OE	17.8	6.1	0.3
ID-c2	〃	10.5	5.5	0.5
ID-c3	〃	27.1	10.7	0.4
ID-c4	TE	9.0	4.0	0.5
TH-c1	NE	8.3	5.3	0.6
TH-c2	〃	7.3	7.7	1.1
TH-c3	〃	5.3	3.8	0.7

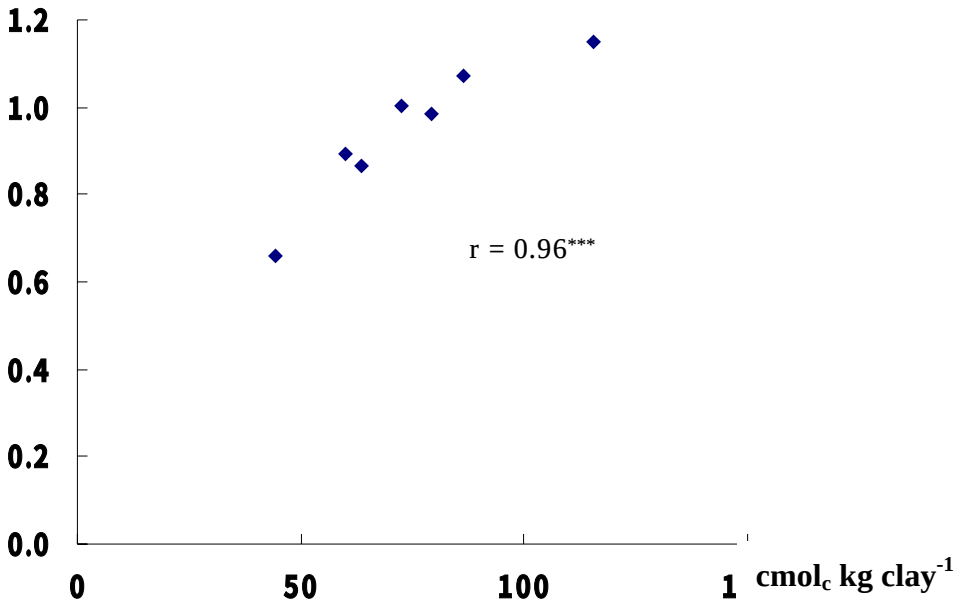

Fig. 3.7. Relationship between CEC per clay and desorption ratio for Ukraine soils.

3.3.3 Cs adsorption-desorption for continuous flow method

1) Effect of ion strength on Cs adsorption-desorption

UA-f2, JP-f1, and TH-c1 were selected as representative samples of the OE, TE, and NE groups, respectively, based on XRD patterns and Cs desorption ratio determined in the batch experiment. They were analyzed for Cs adsorption and desorption kinetics using the continuous flow method. Figure 3.7 represents cumulative adsorption and desorption of Cs^+ with time course. The values of adsorption and desorption maximum (***a***), rate constant (***k***), and Cs desorption ratio are presented in Table 3.4. Figure 3.7 also shows influence of ionic strength (I = 0.8*10^{-3} and 8 *10^{-3}) on the adsorption / desorption kinetics.

The Cs adsorption characteristics determined for CsCl solution at I = 0.8*10^{-3} showed that the rate constant, ***k***, was similar in all the samples (0.11 to 0.12 min^{-1}). It is told that mineralogical compositions normally play an important role in determining rate of ion exchange reactions of soils and the Cs adsorption rates on Ca-saturated kaolinite, smectite, and illite are usually quite rapid, while on vermiculite, it is very slow (Sparks 1989). In this study, however, difference in mineralogical composition did not affect on the rate of Cs adsorption on the Ca-saturated soils.

Not like in the case of rate constant, the value of adsorption maximum, ***a***, of TH-c1 (NE) (9.7 mg kg^{-1}) was smaller than the others (13.1 and 13.2 mg kg^{-1} for UA-f2 (OE) and JP-f1 (TE), respectively). This might be explained by a higher contribution of variable

negative charge in the TH-c1 soil. On the other hand, UA-f2 and JP-f1 have fairly large amounts of expandable 2:1 phyllosilicates with dominated permanent negative charge. The increase in the value of ***a*** along with increase in *I* from $0.8*10^{-3}$ to $8*10^{-3}$ was actually very small as from 13.1 to 14.4 mg kg^{-1} in UA-f2 and from 13.2 to 14.8 mg kg^{-1} in JP-f1, respectively.

In Cs desorption of the continuous flow method, desorption maximum, ***a***, was lower and the Cs desorption ratio was slightly smaller than those determined by the batch experiment. This may be because of 1) an additional desorption of Cs^{+} from destroyed soil aggregates during vigorous mixing in batch experiment, or 2) dialysis applied for the preparation of Cs-saturated samples in a distilled-water for four days, which may result in "aging effect" (i.e. adsorbed Cs diffused into inner part of non-exchangeable layer with time).

Next, Cs adsorption and desorption experiments were conducted at an increased *I* ($8.0*10^{-3}$). In the UA-f2 (OE) and TH-c1 (NE) soils, both the adsorption and desorption rate constants similarly increased with the increase in *I* (i.e., from 0.11 to 0.29 min^{-1} and from 0.11 to 0.21 min^{-1} in adsorption in UA-f2 and TH-c1, respectively, and from 0.13 to 0.34 min^{-1} and from 0.11 to 0.24 min^{-1} in desorption in UA-f2 and TH-c1, respectively), whereas keeping a constant desorption ratio at around 0.85 and 0.5, respectively (Table 3.4), indicating that the

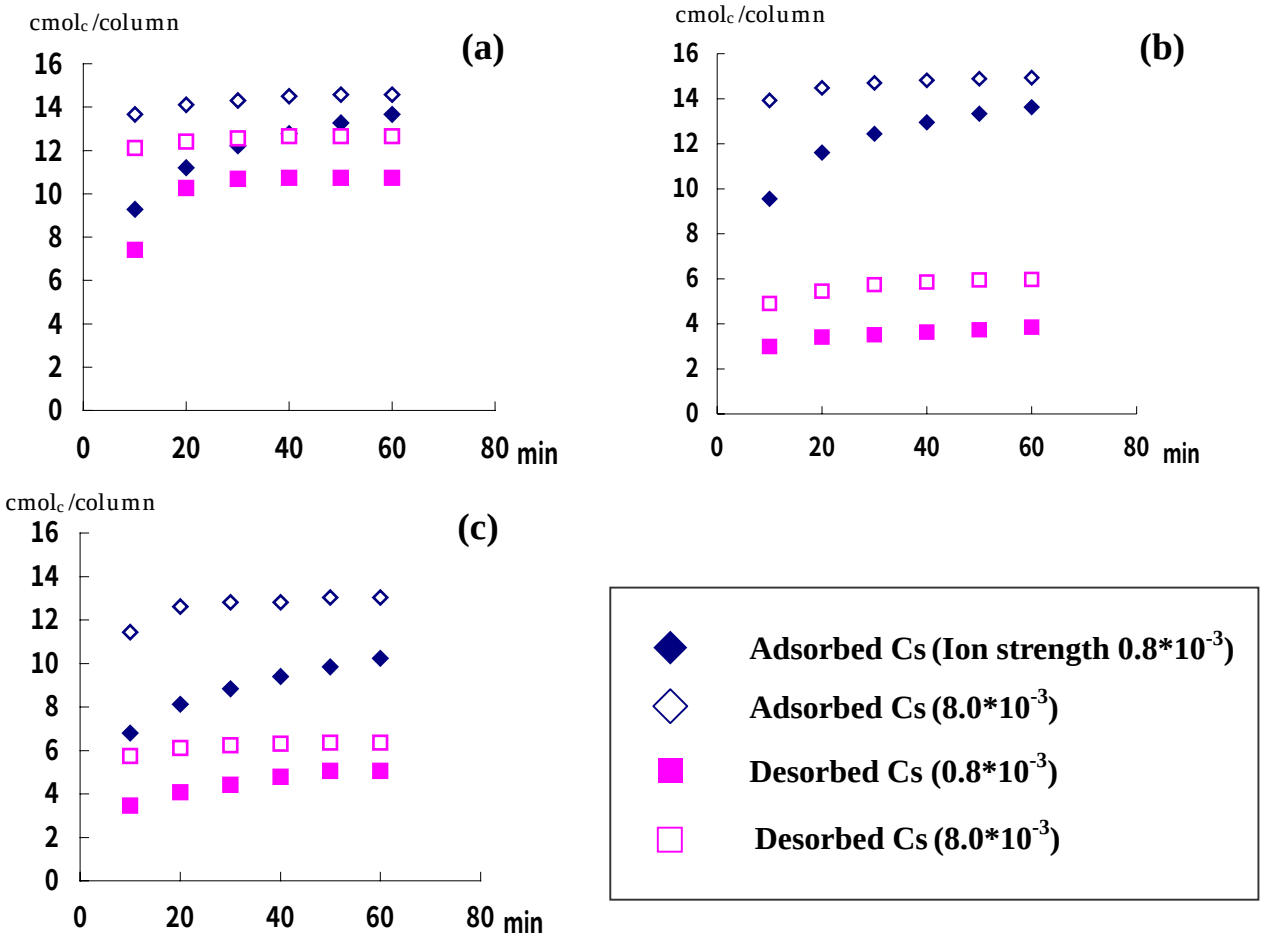

Fig. 3.7. Cumulative amounts of adsorbed- and desorbed-Cs with time in the surface soils at *I* = $0.8*10^{-3}$ or $8.0*10^{-3}$. (a) UA-f2, (b) JP-f1, (c) TH-c1.

adsorption / desorption reactions occur mainly on non-specific adsorption site. In contrast, in JP-f1 (TE), desorption ratio increased (from 0.28 to 0.40) while rate constant kept constant (from 0.16 to 0.17 min^{-1}) along with increase in *I*, suggesting that an additional desorption occurred partially at specific adsorption sites and the adsorbed Cs on the collapsed interlayer sites were, at least to some degree, desorbed when *I* increased from $0.8*10^{-3}$ to $8.0*10^{-3}$. Thus it can be said that FES immobilize Cs independent on *I* of soil solution while collapsed interlayer sites also immobilize Cs but are partially affected by *I*.

2) Difference of Cs adsorption-desorption between surface and subsurface soil

The Cs adsorption and desorption experiments were conducted using subsurface soils of each profile. Subsurface soils were collected just above C horizon in order to minimize the effect of organic matter contents on ion exchange. It would be useful to compare between surface and subsurface soil of each profile in order to analyze the contribution of organic matter on Cs adsorption / desorption reactions.

Table 3.4. Amount of Cs adsorption or desorption maximum (*a*), rate constant (*k*), and desorption ratio (desorption maximum / adsorption maximum) determined for surface soil samples The parameters *a* and *k* are obtained by simulation using first order kinetic equation. Each left value is determined at $I = 0.8*10^{-3}$ and right value is at $I = 8.0*10^{-3}$.

Sample	Adsorption		Desorption		Desorption
(Surface)	*a*	*k*	*a*	*k*	Ratio
UA-f2 (OE)	13.1/14.4	0.11/0.29	10.9/12.6	0.13/0.34	0.83/0.87
JP-f1 (TE)	13.2/14.8	0.12/0.28	3.7/5.9	0.16/0.17	0.28/0.40
TH-c1 (NE)	9.7/12.9	0.11/0.21	4.9/6.3	0.11/0.24	0.50/0.49

Table 3.5. Physicochemical properties of soil samples that are used for continuous flow experiment.

Sample	Depth (cm)	Total C ($g\ kg^{-1}$)	Total N ($g\ kg^{-1}$)	pH (H_2O 1:5)	Clay (%)	CEC (cmolc/kg)
UA-f2 (OE)	0-10	26	3	5.6	26.3	22.7
	120-130	18	0	8.0	19.4	10.8
JP-f1 (TE)	4-22	55	3	3.8	27.0	30.4
	29-50	39	2	4.2	40.7	28.9
TH-c1 (NE)	0-10	23	1	6.1	25.9	13.0
	40-50	12	1	5.3	35.2	19.4

Figure 3.8 comparatively represents cumulative adsorption and desorption of Cs in the surface and subsurface soils with time course. The values of adsorption and desorption maximum (***a***), rate constant (***k***), and Cs desorption ratio for this experiment are presented in Table 3.5. In UA-f2 (OE), the ***k*** value of Cs adsorption in the subsurface soil (0.16 min^{-1}) was larger than surface soil (0.11 min^{-1}) whereas no apparent difference can be seen in the other profiles (0.12 / 0.11 min^{-1} and 0.11 / 0.12 min^{-1} in surface / subsurface soils in JP-f1 (TE) and TH-c1 (NE), respectively). The Cs desorption ratio of subsurface soils was apparently higher than that of surface soils in JP-f1 (0.28 / 0.66 in surface / subsurface soils) and TH-c1 (0.50 / 0.85 in surface / subsurface soils), while such trend was not observed for the UA-f2 soil (0.83 / 0.80 in surface / subsurface soils). The higher values of desorption ratio in the subsurface soils of JP-f1 and TH-c1 are considered to derive from following mechanisms.

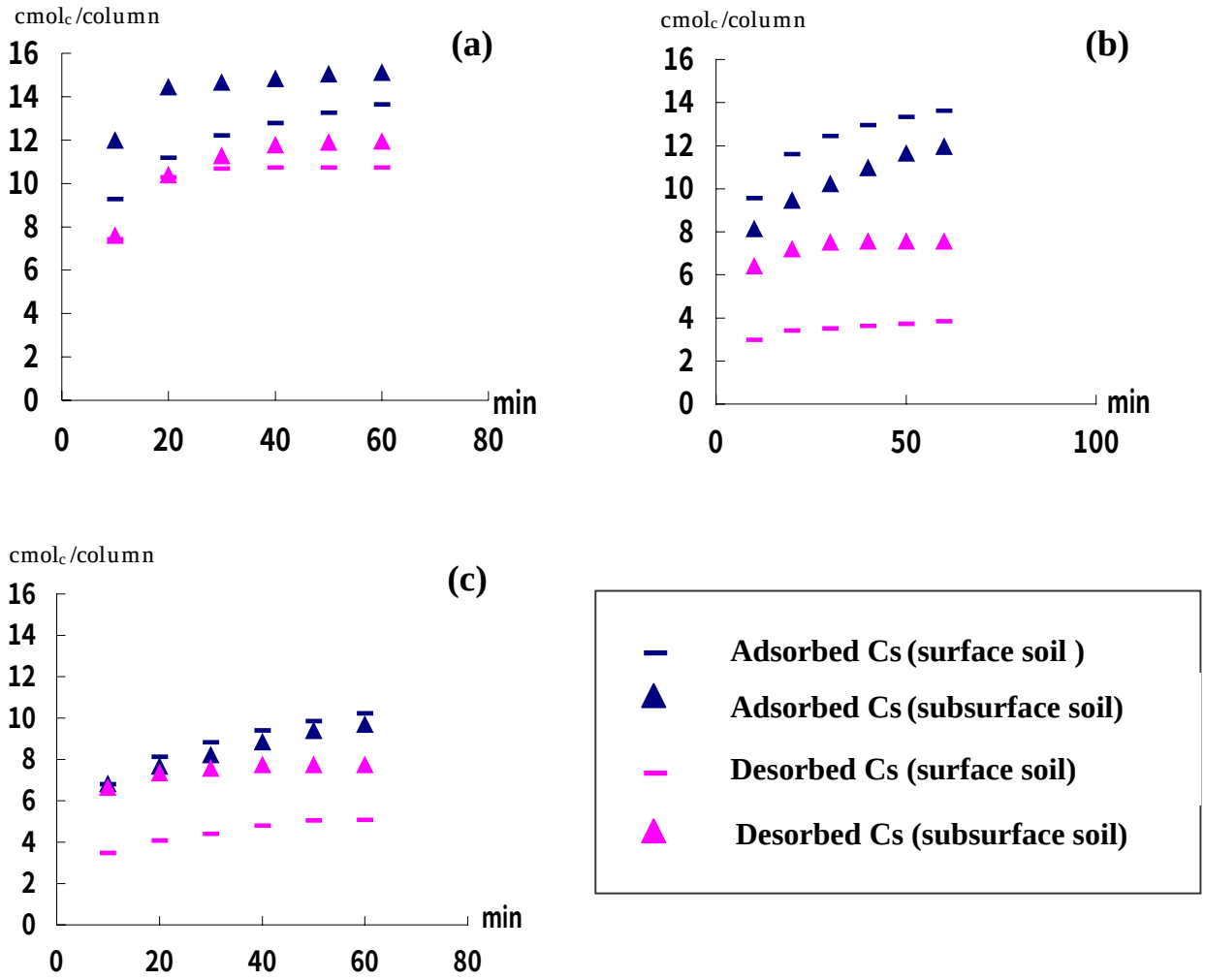

Fig. 3.8. Cumulative amounts of adsorbed- and desorbed-Cs in subsurface soils with time at I = $0.8*10^{-3}$. (a) UA-f2, (b) JP-f1, (c) TH-c1.

The XRD patterns of surface and subsurface soils JP-f1 (TE) has apparently different, that is, most part of 1.4 nm peak of Mg treatment did not move after K treatment in the subsurface soil while that of the surface soil completely collapsed to 1.0 nm after K saturation. This result indicates the presence of HIV in the subsurface soil. In this case, hydroxy-interlayering may be a cause of an increase in desorption ratio through blocking layer changes derived from tetrahedral substitution. On the other hand, mica minerals in the surface soil of TH-c1 (NE) is considered to be more extensively weathered than those in the subsurface, though there is no evident difference in their XRD patterns, resulting in a higher occurrence of FES and hence a lower desorption ratio through Cs immobilization in the surface soil.

Table 3.6. Amount of Cs adsorption or desorption maximum (*a*), rate constant (*k*), and desorption ratio (desorption maximum / adsorption maximum) determined for subsurface soil samples using CsCl or $CaCl_2$ solution with $I = 0.8*10^{-3}$. The parameters *a* and *k* are obtained by simulation using first order kinetic equation.

Sample	Adsorption		Desorption		Desorption
(Subsurface)	*a*	*k*	*a*	*k*	Ratio
UA-f2 (OE)	14.9	0.16	11.9	0.10	0.80
JP-f1 (TE)	11.3	0.11	7.5	0.19	0.66
TH-c1 (NE)	9.1	0.12	7.7	0.20	0.85

Chapter 4
Conclusion

4.1 Weathering sequences of 2:1 minerals under humid climatic conditions in Asia

The *in situ* distribution patterns of clay minerals and thermodynamic analysis of quasi-soil-solution composition reveal the weathering sequence of 2:1 minerals in humid Asia as follows: In moderately to highly weathered soils, dioctahedral mica inherited from parent materials is a major source of 2:1 minerals in soil clays. In Thailand, under moderately acidic conditions with annual precipitation of less than 1500 mm, mica is considered to be directly weathered to kaolin minerals with forming few expandable 2:1 minerals, if any. In contrast, under strongly acidic conditions in Indonesia and/or Japan with higher precipitation, mica tends to firstly weathered to expandable 2:1 minerals and then to kaolinite. Gibbsite can be formed only in initial stage of weathering, if any, in tropics, whereas in Japan fairly large amount of gibbsite and interlayered compounds of Al are formed. The latter components effectively make stable the 2:1 layers through interlayering in spite of ultimate stability of kaolin minerals under humid conditions.

4.2 Cs adsorption and desorption with reference to clay mineralogical composition

Some of the Japanese or Indonesian soils contain fairly large amounts of expandable 2:1 minerals such as vermiculite and/or high charge smectite that can immobilize Cs^+ extensively. In addition to such moderately- to highly-charged expandable 2:1 minerals, FES of weathered mica can immobilize Cs^+ ion. In the soils from Thailand, the Cs immobilizing capacity is not so high and such a FES is mainly responsible for Cs immobilization. On the other hand, the Ukraine soils do not immobilize Cs^+ so extensively because their surface charges are mainly derived from smectite minerals with a low charge density. Therefore, in Ukraine, the Cs immobilizing capacities of soils are relatively small and vary depending on the occurrence of FES in mica minerals.

4.3 Kinetics of Cs adsorption and desorption on soils

At ionic strength of $0.8*10^{-3}$, both the rates of Cs adsorption on Ca-saturated soil and of Cs desorption from Cs-saturated soil are rapid. These reactions attained to the equilibrium state within 60 min. The mineralogical composition does not affect on the difference in rate constants in this study. Judging from the results obtained for Cs-adsorption and desorption behaviors under different ionic strengths (I = $0.8*10^{-3}$ and I = $8*10^{-3}$), FES immobilize Cs independently of I of a soil solution while collapsed interlayer sites also immobilize Cs but

are, to some degree, affected by *I*, i.e., increased ionic concentration of surrounding solution may enhance desorption of Cs^+ once immobilized. Such properties of clay minerals on Cs adsorption are possibly modified through soil formation, i.e., hydroxy-interlayering and/or extensive weathering of mica minerals.

4.4 Available strategy for removing ^{137}Cs from soils in different climatic conditions

Among the soils studied, the low-charge smectites dominated by octahedral isomorphic substitution did not retain Cs^+ irreversibly whereas expandable 2:1 minerals with modelately- to highly-charged layers can immobilize Cs^+ most strongly. The latter minerals are often derived from dioctahedral mica through extensive weathering under humid climates. This is the case that occurs in Japan and/or Indonesia among the present study. Fortunately such soils in Japan are mostly modified by hydroxy-interlayering, which can decrease the chance of irreversible Cs immobilization. Moreover, the Cs^+ ion once immobilized in the collapsed layers of expandable 2:1 minerals can be desorbed if solution *I* increases. In this sense, there is a room for trying phytoremediation in Japanese and/or Indonesian soils although high dose of soluble salts may be required if the main target for extraction of Cs^+ is collapsed 2:1 layers. On the other hand, FES of weathered mica can fix Cs^+ ion independently of solution *I*. In turn, small amounts of ^{137}Cs ion once retained by mica minerals would not be released easily by the change of *I* of surrounding solution. In the soils of Ukraine and Thailand, such mica minerals are considered to be mainly responsible for Cs immobilization. It is, therefore, quite difficult to remove Cs^+ ion from these soils if a fairly large amount of mica minerals are present.

References

Adams, F., 1971: Ionic concentrations and activities in soil solutions. *Soil Sci. Soc. Am. Proc.*, 35, 420-426.

Anderson, S.J. and Sposito, G. 1991: Cesium-adsorption method for measuring accessible structural surface charge. *Soil Sci. Soc. Am. J.*, 55, 1569-1576.

Araki, S., Kyuma, K., Funakawa, S., Lim, S., Suh, Y., Um, K., 1990. Comparative study of red yellow colored soils of Thailand, China, Korea and Japan. Transaction 14th International Congress of Soil Science, Kyoto.

Araki, S., 1993. Comparative study of Kunigami Mahji and Feichisha Soils in Okinawa Islands among red-yellow soils of the world. *Pedologist*, 37, 113-125.

Araki, S., Msanya, B.M., Magogo, J.P., Kimaro, D.N., and Kitagawa, Y., 1998: Characterization of soils on various planation surfaces in Tanzania. Proceeding of World Congress of Soil Science, Montpellier, France.

Avery, S.V. 1996: Fate of Cesium in the Environment: Distribution between the abiotic and biotic components of Aquatic and terrestrial ecosystem. *J. Environ. Radioactivity*, 30, 139-171.

Barshad, I. and Kishk, F.M., 1969: Chemical composition of soil vermiculite clays as related to their genesis. Contributions to Mineralogy and Petrology 24, 136-155.

Borchardt, G. 1989: Smectites. In: Minerals in soil environments, 2nd ed. (eds. J.B.Dixon and S.B Weed), pp. 675-727. Book Series No.1, Soil. Sci. Soc. Am, Madison, WI.

Carlisle, V.W. and Zelazny, L.W., 1973: Mineralogy of selected Florida Paleudults. Soil and Crop Science Society of Florida Proceedings, 33, 136-139.

Cleavert, C.S., Buol, S.W., and Weed, S.B. 1980a: Mineralogical characteristics and transformation of avertical rock-saprolite-soil sequence in the North Carolina Piedmont: Ⅰ. Profile morphology, chemical composition, and mineralogy. Soil Sci. Soc. Am. J., 44, 1096-1103.

Cleavert, C.S., Buol, S.W., and Weed, S.B., 1980b: Mineralogical characteristics and transformation of avertical rock-saprolite-soil sequence in the North Carolina Piedmont: Ⅱ. Feldspar alteration products - Their transformations through the profile. *Soil Sci. Soc. Am. J.*, 44, 1104-1112.

Cook, M.G., 1973: Compositional variations in three typic hapludults containing mica. Soil Sci., 115, 159-169.

Delvaux, B., Kruyts, N., Maes, E., and Smolders, E. 2001: Fate of radiocesium in soil and rhizosphere. *In* Trace elements in the rhizosphere, CRC Press LLC, pp.43-59.

Dixon, J.B. and Schulze, D.G. 2002: Soil mineralogy with environmental applications. SSSA Book series 7, Soil Science Society of America, Inc.

Fanning, D.S., Keramidas, V.Z., and El-Desoky, M.A., 1989: Micas. *In:* Dixon, J.B., Weed, S.B. (Eds.), Minerals in Soil Environments, Book Series No. 1, 2nd ed. Soil Science Society of America, Madison, pp. 551-634.

Funakawa, S., Nambu, K., Hirai, H., Kyuma, K., 1992. Pedogenic acidification process of forest soils in Northern Kyoto. *Soil Sci. Plant Nutr.*, 39, 677-690.

Furian, S.F., Barbiero, L., Boulet, R., Curmi, P. Grimaldi, M, and Grimaldi, C., 2002: Distribution and dynamics of gibbsite and kaolinite in an Oxisol of Serra do Mar, southeastern Brazil. *Geoderma*, 106, 83-100.

Gregory, F. and Carlson, R.M. 1987: Effects of rubidium, cesiumu, thallium on interlayer potassium release from Transvaal vermiculite. *Soil. Sci. Soc. Am. J.*, 51, 305-308.

Henri 2002: Chernobyl-Assessment of radiological and health Impacts. Report of OECD nuclear energy agency.

Hirai, H., Yoshikawa, K., Funakawa, S., Kyuma, K., 1991. Characteristics of bwn forest soils developed under different bio-climatic conditions in the Kinki district with special reference to their pedogenetic processes. *Soil Sci. Plant Nutr.*, 37, 639-649.

Hird, A.B., Rimmer, D.L., and Livens, F.R. 1996: Factors affecting the sorption and fixation of caesium on acid organic soil. *European J. Soil Sci.*, 47, 97-104.

Hodges, S.C., 1987: Aluminum speciation, A comparison of five methods. *Soil Sci. Soc. Am. J.*, 51, 57-64.

Huang, P.M., Wang, M.K., KampF, N., and Schulze, D.G., 2002: Aluminum hydoroxides. *In:* Dixon, J.B., Schulze, D.G. (Eds.), Soil Mineralogy with Environmental Applications, Book Series No. 7, Soil Science Society of America, Madison, pp. 261-289.

Klobe, W.D. and Gast, R.G. 1970: Conditions affecting cesium fixation and sodium entrapment in hydrobiotite and vermiculite. *Soil. Sci. Soc. Am. J.*, 34, 746-750.

Knatko,V.A., Skomorokhov, A.G., Asimova, V.D., Strakh, L.I., Bogdanov, A.P., and Mironov, V.P. 1996: Characteristics of ^{90}Sr, ^{137}Cs, and $^{239, 240}$Pu migration in undisturbed soils of Southern Belarus after the Chernobyl accident. *J. Environ. Radioactivity*, 30 (2), 185-196.

Komarneni, S. 1978: Cesium sorption and desorption behavior of kaolinites. *Soil Sci. Soc. Am. J.*, 42, 531-532.

Kruyts, N and Delvaux, B. 2002: Soil organic horizons as a major source for radiocesium biorecycling in forest ecosystems. *J. Environ. Radioactivity*, 58, 175-190.

Iwasa, Y., 1977: Geographical distribution of clay mineral composition of residual soils in various regions of humid climate. *J. Clay Sci. Soc. Japan*, 3, 75-87.

Jackson, M.L., 1959: Frequency distribution of clay minerals in major great soil groups as related to the factors of soil formation. *Clays Clay Miner.*, 6, 133-142.

Jackson, M.L., 1963: Aluminum bounding in soil. A Unifying principle in soil science. *Soil Sci. Soc. Am. Proc.*, 27, 1-10.

Karathanasis, A.D., 2002: Mineral equilibria in environmental soil systems. In: Dixon, J.B., Schulze, D.G. (Eds.), Soil Mineralogy with Environmental Applications, Book Series No. 7, Soil Science Society of America, Madison, pp. 109-151.

Karathanasis, A.D., Adams, F., Hajek, B.J., 1983: Stability relationships in kaolinite, gibbsite, and Al-interlayered vermiculite soil systems. Soil Sci. Soc. Am. J., 47, 1247-1251.

Kittrick, J.A., 1973. Mica-derived vermiculites as unstable intermediates. *Clays Clay Miner.*, 21, 479-488.

Lasaga, A.C., 1998: Kinetic theory in the earth sciences, Princeton University Press, Princeton.

Lindsay, W.L., 1979: Aluminum, Silica, Aluminosilicate. *In:* Chemical Equilibria in Soils, John Wiley and Sons, Inc. New York, pp. 34-77.

Livens, F.R., Howe, M.T., Hemingway, J.D., Goulding, K.W.T., and Howard, B.J. 1996: Forms and rates of release of ^{137}Cs in two peat soils. *European J. Soil Sci.*, 47, 105-112.

Maes, E., Iserentant, A., Herbauts, J., and Delvaux, B 1999b: Influence of the nature of clay minerals on the fixation of radiocaesium traces in an acid brown earth-podzol. *European J. Soil Sci.*, 50, 117-125.

Maes, E., Vielvoye, L., Stone, W., and Delvaux, B. 1999a: Fixation of radiocaesium traces in a weathering sequence mica → vermiculite → hydroxy interlayered vermiculite. *European J. Soil Sci.*, 50, 107-115.

Mahmoud A.A. Aslani, S.A., Akyil, S., Yaprak, G., Yener, G., and Eral, M 2003: Activity concentration of caesium-137 in agricultural soils. *J. Environ. Radioactivity*, 65, 131-145.

Nettoleton, W.D., Nelson, R.E., and Flach, K.W., 1973: Formation of mica in surface horizons of dry land soils. *Soil Sci. Soc. Am. Proc.*, 37, 473-478.

Nootfleet, M.L., Karathanasis, and A.D., Smith, B.R., 1993: Soil solution composition relative to mineral ditribution in Blue Ridge Mountain Soils. *Soil Sci. Soc. Am. J.*, 57, 1375-1380.

Ogg, C.M. and Backer, J.C., 1999: Pedogenesis and origin of deeply weathred soils formed in alluvial fans of the Virginia Blue Ridge. Soil Sci. Soc. Am. J., 63, 601-606.

Ohta, S., Effendi, S., 1992. Ultisols of lowland Dipterocarp frest in East Kalimantan, Indonesia. **III**. Clay minerals, free oxides, and exchangeable cations. *Soil Sci. Plant Nutr.*, 39, 1-12.

Rai, D. and Kittrick, J.A., 1989: In: Dixon, J.B., Weed, S.B. (Eds.), Minerals in Soil Environments, Book Series No. 1, 2nd ed. Soil Science Society of America, Madison, pp. 161-198.

Rausell-Colon,J.A., Sweatman, T.R., Wells, C.B., Norrish, K., 1965. Studies in the artificial weathering of mica. *In:* Hallsworth, E.G., Crawford (Eds.), Experimental peology, Butterworths, London.

Rebertus, R.A. and Buol, S.W., 1985: Iron distribution in a developmental sequence of soils from mica gneiss and schist. *Soil Sci. Soc. Am. J.*, 49, 713-720.

Rebertus, R.A., Weed, S.B., and Buol, S.W., 1986: Transformations of biotite to kaolinite during saprolite-soil weathering. *Soil Sci. Soc. Am. J.*, 50, 810-819.

Reid-Soukup, D.A and Ulery, A. L., 2002: Smectites. *In:* Dixon, J.B., Schulze, D.G. (Eds.), Soil Mineralogy with Environmental Applications, Book Series No. 7, Soil Science Society of America, Madison, pp. 467-499.

Rosen, K., Oborn, I., and Lonsjo, H. 1999: Migration of radiocaesium in Swedish soil profiles after the Chernobyl accident, 1987-1995. *J. Environ. Radioactivity*, 46, 45-66.

Rosso, K.M., Rustad, J.R., and Bylaska, E.J. 2001: The Cs/K exchange in muscovite interlayers: an *ab initio* treatment. *Clays Clay Miner.*, 49, 500-513.

Seaman, J.C., Meehan, T., and Bertsch, P.M. 2001: Immobilization of cesium-137 and uranium in contaminated sediments using soil amendments. *J. Environ. Qual.*, 30, 1206-1213.

Skopp, J. and McCallister, D. 1986: Chemical kinetics from a thin disc flow system: Theory. *Soil. Sci. Soc. Am. J.*, 50, 617-623.

Sparks, D.L. 1982: Comparison of batch and miscible displacement techniques to describe potassium adsorption kinetics in Delaware soils. *Soil. Sci. Soc. Am. J*, 46, 875-877.

Sparks, D.L. 1987: Kinetics of soil chemical processes. Academic Press, Inc.

Sparks, D.L. 1995: Environmental soil chemistry, Academic Press, Inc.

Springob, G. and Richter, J. 1998a: Measuring interlayer potassium release rates from soil materials. Ⅰ. Critical evaluation on the use of resin and other batch procedures for determining kinetic data. *Z. Pflanzenernahr. Bodenk.*, 161, 315-322.

Springob, G. and Richter, J. 1998b: Measuring interlayer potassium release rates from soil materials. Ⅱ. A percolation procedure to study the influence of the variable ‘solute K’ in the <1-10 μM range. *Z. Pflanzenernahr. Bodenk.*, 161, 323-329.

Van Breemen, N. and Brinkman, R. 1976: Chemical equilibria and soil formation. *In:* Bolt, G.H., Wruggenwert, M.G.M. (Eds.) Soil Chemistry, A. Basic elements, Elsevier Scientific publishing company, Amsterdam.

Wolt, J.D., 1994: Mineral stability and pedogenesis. *In:* Soil Solution Chemistry, Applications to environmental science and agriculture, John Wiley and Sons, Inc, New York, pp. 181-208.

Yoshinaga, N., Kato, Y., Nakai, M., 1989. Mineralogy of red- and yellow-colored soils from Thailand. *Soil Sci. Plant Nutr.*, 35, 181-205.

Zelazny, L.W., Carlisle, V.W., and Calhoun, F.G., 1975: Clay mineralogy of selected Paleudults from the Lower Coastal Plain. In: ASA, Agronomy abstracts, Madison.Springob, G. 1999: Blocking the release of potassium from clay interlayers by small concentrations of NH_4^+ and Cs^+. *European J. Soil Sci.*, 50, 665-674.